Vol. 16: 79–99, 2001 | CLIMATE RESEARCH Clim Res | Published January 18

The atmospheric response to a reduction in summer Antarctic sea-ice extent

D. A. Hudson*, B. C. Hewitson

Department of Environmental and Geographical Science, University of Cape Town, Private Bag, Rondebosch, 7701, South Africa

ABSTRACT: This paper examines the response of an atmospheric general circulation model (GCM) to a reduction in Antarctic sea-ice extent during summer. The control simulations are forced by prescribed, observed sea surface temperatures (SSTs) and sea-ice extents, while in the perturbation simulations sea-ice is reduced. The simulations are restarts of an AMIP (Atmospheric Model Intercomparison Project) configured simulation, and 2 summers (1979/80 and 1984/85) were selected for the study. The results show that a reduced sea-ice extent causes an increase in surface air temperatures in the regions where sea-ice was removed, and an associated decrease in pressure at high latitudes (around 60° S). The greatest increase in surface air temperatures are found north of the Weddell and Ross Seas. There is an increase in pressure between 30 and 50° S, which is associated with a strengthening and southward extension of the subtropical high pressure belt. The change in vertical velocities supports these results showing an intensification of the ascending limb of the Ferrel cell and a southward extension of the descending limb of the Hadley cell. In response to the perturbation there is an increase in wind speeds in mid/high latitudes (45 to 65° S), and a decrease in the westerly flow in the subtropics (30 to 40° S). The amplitude of circumpolar wave number 1 decreases in the perturbations compared to the controls in both years. This may be a result of reduced asymmetry of the SST distribution about the pole and the southward shift of the subtropical high-pressure belt. A cyclone analysis shows an increase in the number of midlatitude cyclones around Antarctica (60 to 70° S) and a decrease further north (40 to 60° S). The general pattern of changed circulation for the summer of 1984/85 is positioned slightly south of that in 1979/80, perhaps related to the less extensive sea-ice in 1984/85.

KEY WORDS: Antarctic sea-ice extent · General circulation model · Climate response

1. INTRODUCTION

There is substantial evidence that sea-ice can force changes in atmospheric circulation in the region of the sea-ice margin (e.g. Ackley & Keliher 1976, Ackley 1981, Carleton 1981, Streten 1983, Mayes 1985, Watkins & Simmonds 1995), but of more interest is the suggestion that sea-ice variations around Antarctica can cause an atmospheric response in the midlatitudes and subtropics, as well as in polar and subpolar latitudes. In contrast to the Arctic, Antarctic sea-ice has an outer boundary which is unconstrained by land, and therefore interacts both dynamically and thermodynamically with the atmospheric and oceanic circulation of mid- and lower latitudes of the southern hemisphere (Carleton 1992). The seasonal cycle of Antarctic sea-ice displays large changes in ice extent, in addition to considerable interannual variability. The controls of this interannual variability are not well known (Hanna 1996), and we still do not have a good understanding of the influence which these present-day Antarctic sea-ice variations exert on the climate, especially non-polar climates. This paper addresses the question of how an anomalously reduced sea-ice extent (reduced either in the future in response to global warming, or as a consequence of interannual variability) would impact hemispheric and synoptic atmospheric circulation patterns.

*E-mail: hudson@egs.uct.ac.za

The analysis of observed data is of limited use when attempting to investigate such a question, since the relationships found between the observed seasonal behaviour of sea-ice extent and some atmospheric variable may not necessarily be the same as a response of that variable to sea-ice anomalies within a given season. In addition, with statistical studies using observed data, it is often difficult to establish cause and effect. An ice anomaly itself is the response to atmospheric forcing, and therefore determining the ice's subsequent influence on the atmosphere is problematic. It is also possible that the atmospheric response to sea-ice is non-linear, and therefore one should be cautious in interpreting the results from studies with observed data that use linear statistical methods, such as correlations. Thus, the approach adopted in the current study is to use a general circulation model (GCM) in order to isolate the effect of prescribed anomalies of sea-ice extent.

The present study utilises a GCM which is forced with prescribed sea surface temperatures (SSTs) and sea-ice extents, where the fields in the control simulation are from observational data and are subsequently perturbed in the experiment. By using prescribed fields, one is able to isolate the forcing from the sea-ice perturbation; in contrast, results from a GCM using a sea-ice model would be complicated by feedback between the atmosphere and sea-ice, and the effect of the sea-ice on the atmosphere would be more difficult to determine. By nature of the model used, the sea-ice reduction experiments cannot take into account the subsequent feedback of the atmosphere to the ocean or cryosphere.

A number of modelling experiments investigating the atmospheric response to a reduction in sea-ice have been performed for the Arctic (Fletcher et al. 1973, Newson 1973, Warshaw & Rapp 1973, Herman & Johnson 1978, Serafini & Le Treut 1988, Dümenil & Schröder 1989, Raymo et al. 1990, Royer et al. 1990, Crowley et al. 1994, Murray & Simmonds 1995). However, results obtained from studies with the Arctic are not necessarily transferable to the Antarctic, primarily due to the different distribution of land masses in the hemispheres. In addition, the seasonal variation of sea-ice cover is about 6 times greater around Antarctica than in the Arctic (Simmonds 1981). The southern hemisphere experiments that have been performed can be grouped into those examining the impact of reduced sea-ice concentration, on the one hand, and reduced sea-ice extent on the other. In terms of sea-ice concentration, Ledley (1988) used an energy balance climate model coupled to a 3-layer thermodynamic sea-ice model to investigate the feedback between atmospheric temperature and small areas of open ocean (leads) within the winter sea-ice zone. Ledley found that due to changes in the sensible heat flux, leads have a large impact on the atmospheric temperature of polar regions. Similarly, Simmonds & Budd (1990, 1991) examined the response of the atmosphere to changes in the open water fraction of Antarctic sea-ice in perpetual July simulations with an R21 spectral resolution GCM using prescribed SSTs and sea-ice extents. They also found substantial atmospheric warming in those areas where leads were included, and the experiments appeared to indicate westerly wind anomalies south of 60° S and anomalous easterlies between 40 and 60° S in response to reduced sea-ice concentrations. Simmonds & Wu (1993) extended the previous research by examining the effect of reduced sea-ice concentrations on midlatitude cyclones. They found a general tendency for an increase in the number of cyclones surrounding the Antarctic continent and a decrease further north, as well as enhanced cyclogenesis south of about 65° S, especially over the western Weddell Sea. In contrast to the above studies, Watkins & Simmonds (1995) performed a number of short simulations (5 d) using an R31 spectral resolution GCM with prescribed SSTs and sea-ice extents in order to determine the atmospheric response to Antarctic sea-ice concentrations on synoptic time scales. The results suggested that real-time Antarctic sea-ice data may be particularly useful for numerical weather prediction.

In contrast to varying Antarctic sea-ice concentration, there have been a number of studies which, as is the focus in the present study, have modified sea-ice extent. Simmonds (1981) replaced September sea-ice extent with that for March in a perpetual September simulation using a hemispheric GCM. In another study, Mitchell & Hills (1986) examined the effect of removing all Antarctic sea-ice equatorward of 66° S and replacing it with water at 0°C. To do this they performed three 4 mo (June, July, August, September) GCM replicate experiment simulations. In response to the latter paper, Simmonds & Dix (1987) expanded upon the 1981 research (Simmonds 1981), using a global version of the same GCM as before, although with some improvements. In a perpetual July simulation, they removed all sea-ice in the experiment and replaced it with open water at 0°C. Lastly, Mitchell & Senior (1989) repeated the experiments of Mitchell & Hills (1986) using an 11-layer GCM in order to produce an improved control simulation. In response to the various imposed winter sea-ice extent reductions, all the above studies (Simmonds 1981, Mitchell & Hills 1986, Simmonds & Dix 1987, Mitchell & Senior 1989) found a decrease in the zonally averaged westerly component of the wind between about 45 and 65° S in the mid- to upper troposphere. In addition, they all noted zonally averaged warming of the lower tropo-

sphere south of about 55°S as a result of the sea-ice reduction. Mitchell & Hills (1986) and Mitchell & Senior (1989) showed that the increase in surface temperature caused an increase in both sensible and latent heat fluxes in the zone from which sea-ice was removed, with decreases just to the north of this zone. There are, however, a number of inconsistencies between the results of the different experiments, especially in terms of the sea level pressure response.

The abovementioned experiments were conducted with large and sometimes unrealistic sea-ice extent anomalies. The removal of ice north of a designated latitude (Mitchell & Hills 1986, Mitchell & Senior 1989) does not take into account asymmetrical melting around the Antarctic continent, such as the substantial seasonal ice changes that occur in the region of the Ross and Weddell Seas (Ackley 1981). It is also unrealistic for the sea-ice distribution in the experiment simulation to remain constant from June through to September, as was the case in the studies by Mitchell & Hills (1986) and Mitchell & Senior (1989). Furthermore, these experiments, together with those of Simmonds (1981) and Simmonds & Dix (1987), imposed extreme changes in sea-ice extent, and one should be cautious in applying the results to the smaller perturbations in ice extent that are actually observed. In these types of studies there is, however, the problem of what anomalous sea-ice data set to introduce into the model. In the current study, an algorithm, devised by Hudson (1999), has been used to generate sea-ice data sets for experiment simulations similar to those mentioned above. For any given month of the GCM control sea-ice data set, the algorithm will produce a corresponding month with reduced sea-ice coverage, which can be used in the experiment simulation. The sea-ice perturbations that are introduced to the model in this study resemble the magnitude of interannual differences in sea-ice extents. In addition, the abovementioned studies all focussed on the winter season, and the effects of a reduction in Antarctic sea-ice extent in the summer season have not been considered. For this reason, the present study will address the summer season. In summer the atmospheric circulation at mid- to high southern latitudes is less energetic and variable compared to winter; therefore it is likely that the sea-ice - atmosphere signal-to-noise ratio would be greater.

2. DESCRIPTION OF THE MODEL

The present study uses the latest version of the GENESIS (Global Environmental and Ecological Simulation of Interactive Systems) GCM (version 2.0.a), which was developed at the National Center for Atmospheric Research (NCAR). The model originated from an effort to develop a first-generation earth system model which especially emphasises terrestrial physical, biophysical and cryospheric processes (Thompson & Pollard 1995, 1997). GENESIS has been widely used by climatologists and has found a particular niche in paleoclimate modelling (Barron et al. 1993, 1995, Crowley et al. 1993, 1996, Otto-Bliesner 1993, Crowley & Baum 1994, Foley 1994, Jenkins 1995). Since the model has been used extensively for paleoclimatic experiments, it is one of the few GCMs that has been found to be satisfactory under a climate regime other than the present day. Studies with GENESIS version 2.0.a have included an examination of Greenland and Antarctic mass balances for the present-day and doubled-CO_2 situations (Thompson & Pollard 1997), an analysis of the density, distribution and characteristics of midlatitude cyclones over the oceans south of Africa (Hudson & Hewitson 1997) and an investigation into the climatic response over southern Africa and adjacent oceans to a doubling of CO_2 in the model (Hudson 1997).

In the current application of the model the atmospheric component is coupled to multi-layer models of vegetation, soil, land-ice and snow, and uses prescribed SSTs and sea-ice extents. The atmospheric model has a T31 spectral resolution with 18 atmospheric levels, and is coupled to the 2° by 2° land surface models by means of a Land-Surface-Transfer (LSX) scheme. A detailed description of GENESIS version 2.0.a is provided by Thompson & Pollard (1997), and the previous version (1.02) of the model has also been described by Pollard & Thompson (1994, 1995a) and Thompson & Pollard (1995).

3. SEA-ICE ALGORITHM

The sea-ice algorithm is used for the present study in order to facilitate the generation of sea-ice perturbation data sets that are fairly realistic, in that the sea-ice reductions are not applied uniformly around the Antarctic continent, and data sets of multiple months can be obtained where a realistic seasonal cycle is clearly evident. The latter permits simulations where the sea-ice distribution changes from month to month, in keeping with the seasonal cycle, rather than having a fixed sea-ice distribution over the multi-month simulation period or using a perpetual simulation, as has been done in the past. The severity of the perturbation can also be varied, depending on the purpose of the study. Where sea-ice was removed in previous modelling studies (Simmonds 1981, Mitchell & Hills 1986, Simmonds & Dix 1987, Mitchell & Senior 1989), it was replaced with a constant temperature, less than or equal to 0°C, depending on the study. However, in the present study in those regions where sea-ice is re-

moved, the adjacent regional SST gradient is extended to the new sea-ice boundary; thus, it includes the effect of the warming of ice-free surface waters, whereas previous studies did not. As well as examining the effect of reduced freezing during winter, the algorithm also facilitates the investigation of the atmospheric impact of enhanced sea-ice melt during the summer months. The procedure for creating perturbation data sets for both summer and winter months is described in detail by Hudson (1999), but a general conceptual overview of the algorithm is given in Appendix 1.

4. EXPERIMENTAL DESIGN

The perturbation and control simulations used to determine the impact of reduced sea-ice limits are embedded in a 10 yr Atmospheric Model Intercomparison Project (AMIP) (Gates 1992) simulation of the model, which is forced by prescribed SSTs and sea-ice extents corresponding to the years extending from 1979 to 1988. The perturbation and control simulations are model restarts of certain portions of the 10 yr period.

The summers of 1979/80 (hereafter referred to as 1980) and 1984/85 (hereafter referred to as 1985) were selected for the study. These periods were selected from the available 10 years because they do not exhibit strong El Niño signals and they appear to have extremes in sea-ice distribution, such that 1980 is characterised by more extensive sea-ice than 1985 (Fig. 1). With regards to the latter, the intention is to determine whether the amount of sea-ice present affects the results.

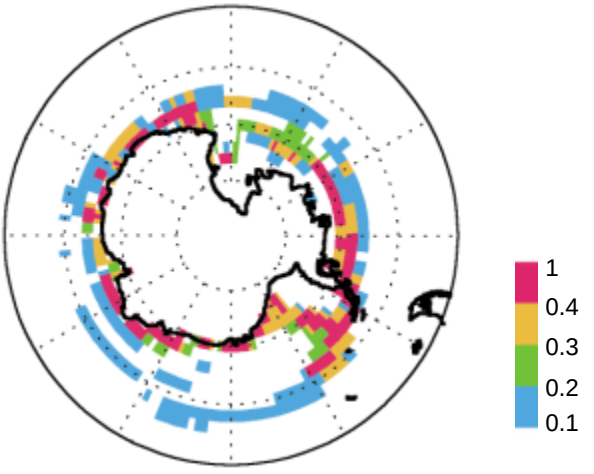

Fig. 1. 1980 sea-ice extent minus 1985 sea-ice extent for the observed data in summer, i.e. averaged over November, December, January, February and March. (Note: for each month in the data set a grid cell is either I or O, denoting ice or ocean, respectively)

A summary of the details of the experimental design is shown in Table 1. An ensemble of 3 integrations has been performed for each period for both the control and perturbation conditions. All of the integrations within an ensemble are forced by the same imposed ice and SST anomaly, but each starts from different initial conditions, i.e. the second and third integrations are started 1 and 2 mo earlier from the extended control run of the model (Table 1). They have to be started months rather than a day or two earlier, because the restart files for the vegetation component of the model are only available for the beginning of each month.

For the control simulations the boundary conditions and restart files saved from the continuous 10 yr simulation are not altered. In contrast, for the perturbations the SST and sea-ice input file is modified, with November, December, January, February and March being perturbed (Table 1). In the model, daily values of SSTs and sea-ice extent are obtained from the monthly input fields by linear interpolation in time from the 2 adjacent mid-month values (Pollard & Thompson 1995b). This implies that, for example, the first half of November's SST and sea-ice field in the perturbation simulations is obtained from interpolation between the unperturbed October field and the perturbed November field. Furthermore, March's SST and sea-ice field has been per-

Table 1. Details of the experimental design, in terms of the months for which sea-ice was perturbed, the months that were included in the simulations and the months that were analysed

Months with perturbed sea-ice in the perturbation simulations	Length of model run (controls and perturbations) 1	2	3	Months analysed
			Sep (1979)	
		Oct (1979)	Oct (1979)	
Nov (1979)	Nov (1979)	Nov (1979)	Nov (1979)	
Dec (1979)	Dec (1979)	Dec (1979)	Dec (1979)	Dec (1979)
Jan (1980)	Jan (1980)	Jan (1980)	Jan (1980)	Jan (1980)
Feb (1980)	Feb (1980)	Feb (1980)	Feb (1980)	Feb (1980)
Mar (1980)				
			Sep (1984)	
		Oct (1984)	Oct (1984)	
Nov (1984)	Nov (1984)	Nov (1984)	Nov (1984)	
Dec (1984)	Dec (1984)	Dec (1984)	Dec (1984)	Dec (1984)
Jan (1985)	Jan (1985)	Jan (1985)	Jan (1985)	Jan (1985)
Feb (1985)	Feb (1985)	Feb (1985)	Feb (1985)	Feb (1985)
Mar (1985)				

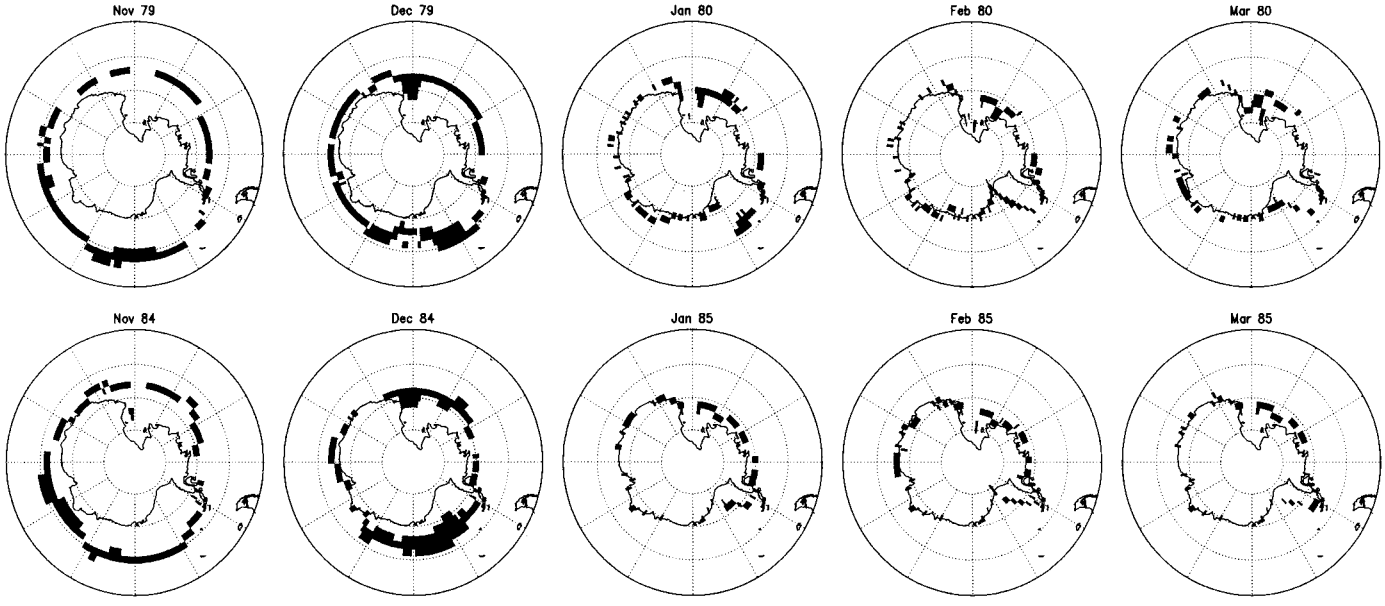

Fig. 2. Difference (control minus perturbed) in the position of the sea-ice margin for the 1979/80 and 1984/85 summer months. Black areas indicate areas from which sea-ice was removed for the perturbation simulation

turbed even though the simulations do not extend to this month (Table 1), so that the latter half of February can use perturbed fields for the interpolation.

Only the last 3 months of the integrations were analysed, i.e. December, January, February (DJF) (Table 1), in order to diminish the problem of the initial jump from observed to perturbed settings and thus allow the model to adapt to the new boundary conditions in the perturbations. Mitchell & Hills (1986), Mitchell & Senior (1989) and Royer et al. (1990) also analysed the data 1 mo after their respective sea-ice perturbations had been introduced. Similarly, the results from other sea-ice sensitivity studies using simulations run in perpetual mode were also based on data subsequent to a period of supposed stabilisation (Simmonds & Dix 1987, Simmonds & Budd 1991, Murray & Simmonds 1995).

The differences between the control and perturbation sea-ice fields that have been used for the experiments are shown in Figs. 2 & 3. A comparison between the average reduction in sea-ice in the perturbations (Fig. 3) and the observed difference in sea-ice extent

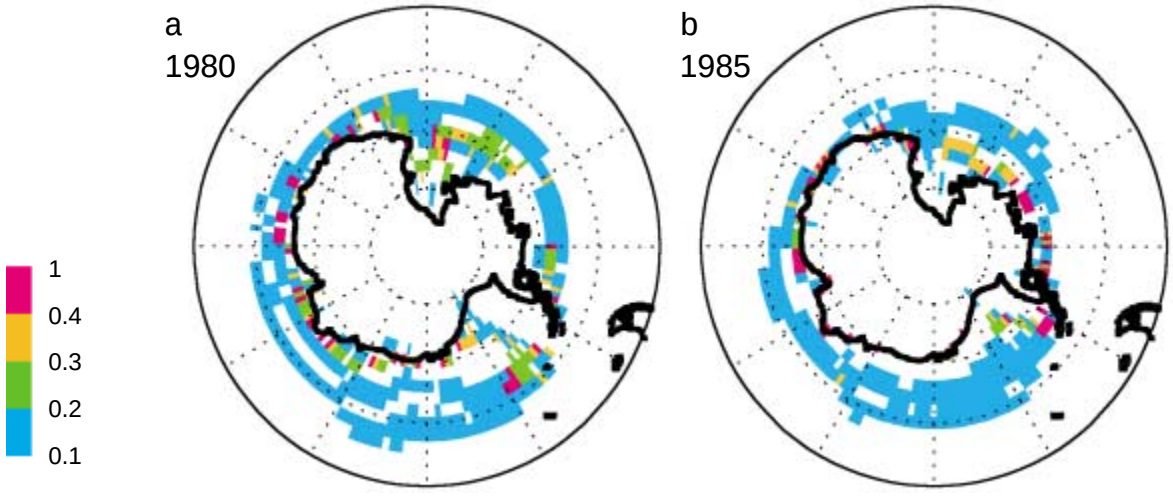

Fig. 3. Control sea-ice extent minus perturbed sea-ice extent for (a) summer 1980, i.e. averaged over November (1979), December (1979), January, February and March, and (b) summer 1985, i.e. averaged over November (1984), December (1984), January, February and March. (Note: for each month in the data set a grid cell is either I or O, denoting ice or ocean, respectively)

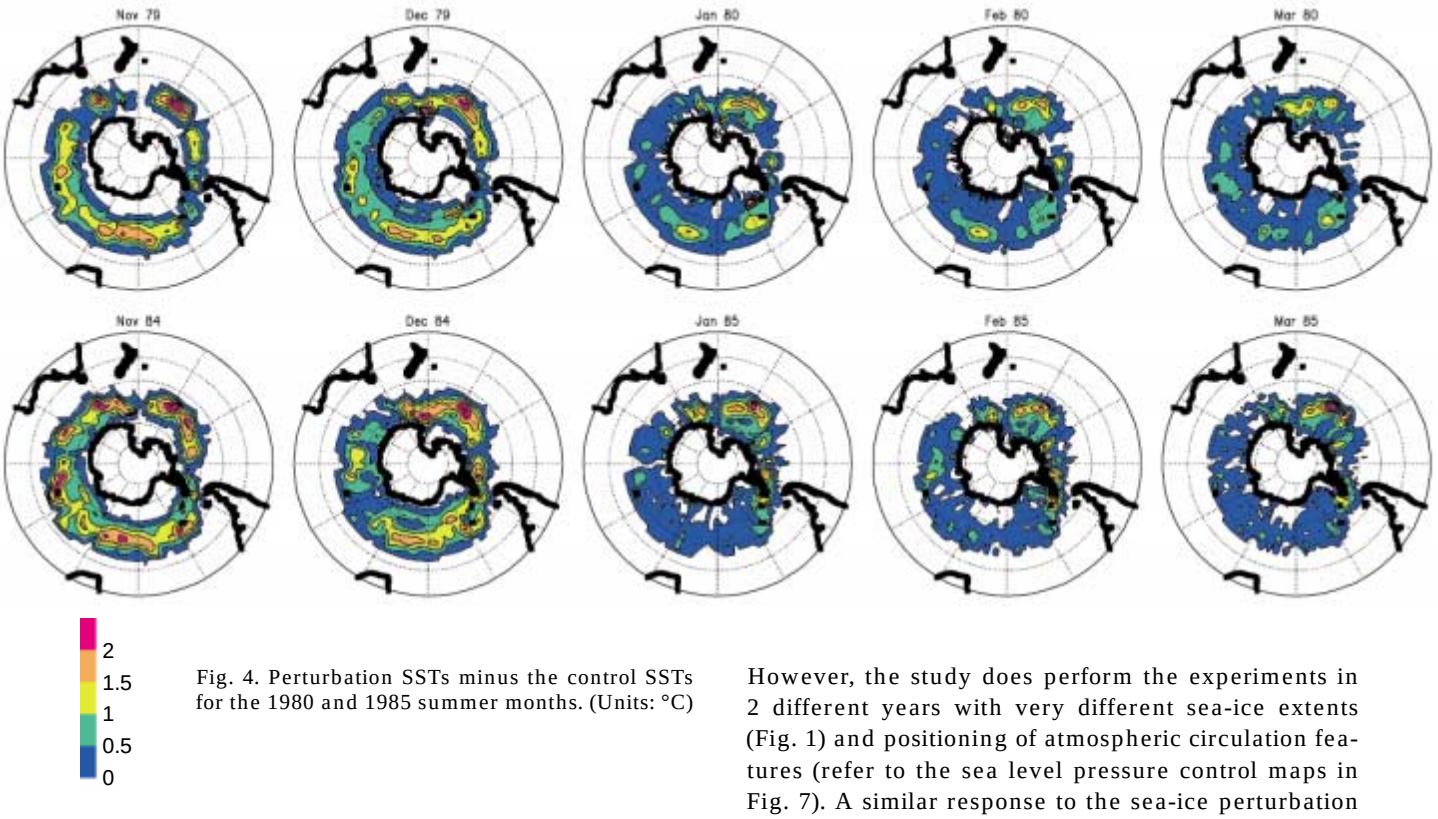

Fig. 4. Perturbation SSTs minus the control SSTs for the 1980 and 1985 summer months. (Units: °C)

between 1980 and 1985 (i.e. an indication of natural variation) (Fig. 1) shows that the anomalies introduced into the model are not unreasonable in terms of spatial pattern and strength. Fig. 4 shows the difference between the observed and perturbed SSTs for each month of the perturbations. SSTs are higher in the perturbations, since in the algorithm when sea-ice is removed, the SST gradient is extended to the new sea-ice boundary, thus warming the ice-free waters.

Lastly, it is important to note that 3 integrations for each experiment situation may not be sufficient to take into account the inherent non-linearity of the atmosphere and reduce the 'noise' associated with natural variability, such that a clear sea-ice - atmosphere response can be detected. This is particularly pertinent to the mid- to high latitudes, where the internal variability of the atmosphere is large. In a review of the ability of GCMs to simulate climate variability in the southern hemisphere, Nicholls (1996) commented that there appears to be too much variability in the models, and that the degree of this internally generated variability means that multiple integrations are needed to obtain reliable simulations. Thus, the restricted number of integrations (i.e. 3) per ensemble is a potential limitation of the present study. It will be shown later that many of the anomalies obtained in response to the perturbation are very small, and it is not always clear which of these changes are due to a true response to the forcing and which due to interannual variability. However, the study does perform the experiments in 2 different years with very different sea-ice extents (Fig. 1) and positioning of atmospheric circulation features (refer to the sea level pressure control maps in Fig. 7). A similar response to the sea-ice perturbation in the 2 years will increase the reliability of the results and our confidence that a true sea-ice signal was detected.

5. RESULTS AND DISCUSSION

5.1. Temperature and pressure

In response to the sea-ice and SST anomalies there is an increase in surface air temperatures, although very small, between about 40 and 65° S in both years (Fig. 5). The increase between 60 and 65° S is probably a direct response to reduced sea-ice limits, whereas the surface increases further north are due to the manipulation of SSTs. Since summer is the season of high insolation in the polar region, the mechanism producing the higher-latitude surface temperature increase is likely to be the lower albedo in the perturbations due to less expansive sea-ice. For example, sea-ice covered with a thick layer of snow has an albedo of about 80 %, whereas the open ocean has an albedo of about 10 % (Budd 1991). The polar temperature increase for 1985 appears to be stronger than that of 1980, and is positioned slightly southward (Fig. 5). This can be related to differences in the perturbations and extent of sea-ice cover in the 2 years. Firstly, the control sea-ice of 1985 is located further poleward (less expansive) than that of 1980, and hence the sea-

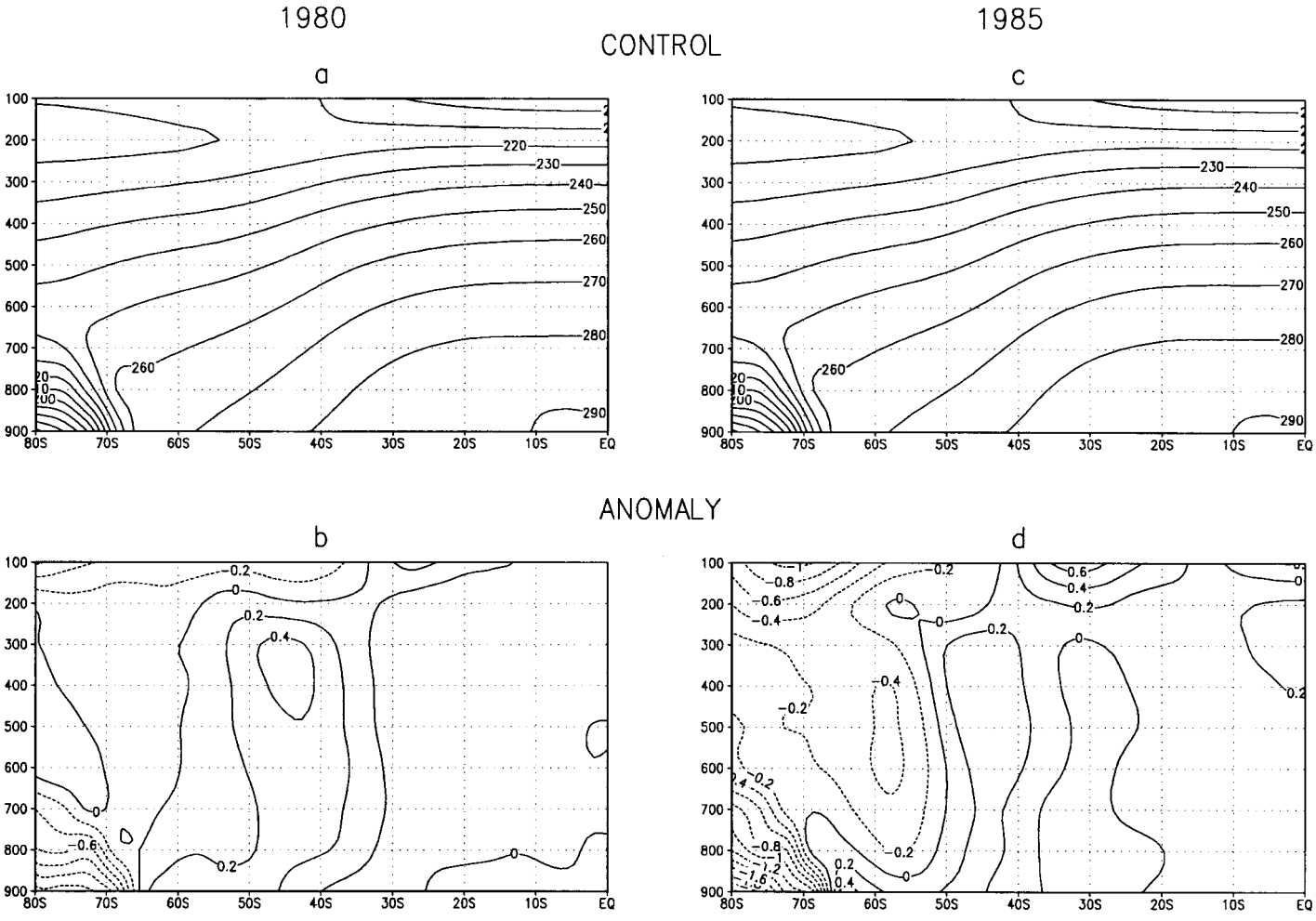

Fig. 5. Vertical cross sections (*y*-axis denotes the pressure level in hPa) of the zonally averaged temperature (K) for the (a) control and (b) anomaly (perturbations minus the controls) of 1980, and the (c) control and (d) anomaly of 1985. (Note: Results displayed in the vicinity of the Antarctic plateau are fictitious, i.e. below ~700 hPa and poleward of ~75° S. They have been artificially generated by interpolation to pressure levels, even though these levels are below the earth's surface)

ice and SST perturbations are located further poleward (Figs. 2 to 4); and secondly, Fig. 2 shows that the largest sea-ice perturbation imposed was for December 1984 (part of the '1985' summer) and perhaps this explains the slightly stronger temperature response in 1985. The high-latitude surface warming in both years does not extend over the Antarctic continent, and in fact the response is that of surface cooling over the land (Fig. 5). Katabatic winds blowing off the plateau may have prevented the penetration of the warmer air over the Antarctic continent. It is important to note, for all the cross sections presented, that the 700 hPa surface actually intersects with much of the Antarctic plateau, and therefore the results displayed in this region below 700 hPa level are likely to be fictitious.

It is clear from the results presented here that the temperature response to the sea-ice perturbation is small and may not be climatically significant. The surface temperature changes obtained are much smaller than those from other modelling studies investigating the effects of reduced winter Antarctic sea-ice extent, which reported temperature increases in the vicinity of the ice removal of about 10 to 20°C (Mitchell & Hills 1986, Simmonds & Dix 1987, Mitchell & Senior 1989). This is not surprising, since the experiments of Mitchell & Hills (1986), Simmonds & Dix (1987) and Mitchell & Senior (1989) made use of considerably larger sea-ice perturbations than the present study, either removing all winter sea-ice (Simmonds & Dix 1987) or removing all sea-ice equatorward of 66 (Mitchell & Hills 1986) or 67.5° S (Mitchell & Senior 1989). In addition, different mechanisms may be more or less important in summer as opposed to winter. In contrast to summer, the important mechanism causing the increase in winter is the modification of heat fluxes, rather than the ice-albedo feedback. The low intensity and oblique angle of insolation diminishes the influence of the surface albedo changes during winter (Raymo et al. 1990). Further-

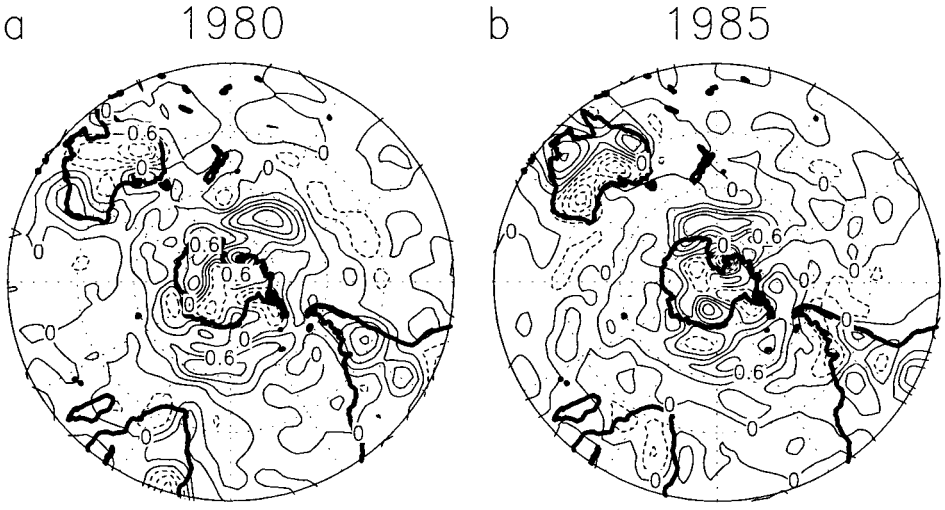

Fig. 6. Surface air temperature (K) anomalies (perturbations minus the controls) for (a) 1980 and (b) 1985. Negative anomalies are depicted as dashed contours, and the contour interval is 0.3 K

more, a weaker temperature response in summer may be because high latitude inversions are generally weaker during summer compared to winter, and therefore in summer there may be a greater potential for the dispersion of low-level temperature anomalies through convection.

The averaged results shown in the cross sections may obscure changes of a regional nature and in certain cases may be misleading since the introduced disturbances are not zonally orientated. The 2-dimensional field response shows that the surface air temperature anomalies south of 50° S (Fig. 6) largely mirror the imposed change in SSTs (Fig. 4), with greatest increases recorded north of the Ross Sea (up to about 1.5 K) and north and northeast of the Weddell Sea (about 0.9 K) in both years (Fig. 6). As with the SST perturbations, the surface temperature increase in these 2 regions is situated slightly more poleward in 1985 compared to 1980. Furthermore, the temperature increase for the Ross and Weddell Sea regions in 1985 is shifted slightly west compared to 1980. These small differences between the 2 years are related to differences in the magnitude and positioning of the imposed sea-ice and SST anomalies (Figs. 2 to 4). For example, if one focuses on the Weddell Sea sector, the SST perturbation in this sector is closer to the pole for 1985 and is also larger directly north of the sea than it is for 1980 (Fig. 4).

The high-latitude temperature increase (Fig. 6) is associated with regions of sea level pressure decrease around Antarctica in both years (Fig. 7), such that the largest falls in pressure generally coincide with the greatest increases in diabatic heating. The decreases in pressure are largest over the Weddell Sea, south Indian and Ross Sea sectors (Fig. 7), where the introduced anomalies in sea-ice extent and SSTs are largest, and give rise to a 3-wave pattern of change, especially for 1980. As mentioned previously, the temperature increase for the Ross and Weddell Sea regions in 1985 is shifted slightly west compared to that in 1980. A similar difference between the 2 years is evident in the sea level pressure anomalies. For example, in 1985 there appears to be a larger increase in surface temperature in the region between South America and the Antarctic Peninsula, and slightly west and east of this area, compared to 1980 (Fig. 6). Similarly, the zone of sea level pressure decrease in the Weddell Sea sector extends westwards past the Antarctic Peninsula in 1985, whereas it does not extend past the peninsula in 1980 (Fig. 7). It thus appears that some of the observed differences in the positioning of the sea level pressure anomalies may be related to differences in the positioning and size of the imposed perturbations in the 2 years.

The sea level pressure decreases around Antarctica (Fig. 7) largely correspond to the patterns of 500 hPa height decreases (Fig. 8) and 500 hPa temperature decreases (not shown) in both years. This suggests that the temperature decrease in the mid-troposphere (Fig. 5) is a response to adiabatic cooling due to increased uplift induced by increased lower-level convergence. This increase in lower-level convergence may have been triggered by the increase in surface temperatures, which are associated with the regions of sea level pressure decrease in both years (Figs. 6 & 7), or by changes in baroclinicity induced by the sea-ice and SST perturbation. The regions of pressure decrease around Antarctica at the 500 hPa level (Fig. 8) are positioned slightly west of the regions of sea level pressure decrease (Fig. 7). This is to be expected, since increasing baroclinicity is accompanied by a signature of westward-sloping axes of pressure minima with height.

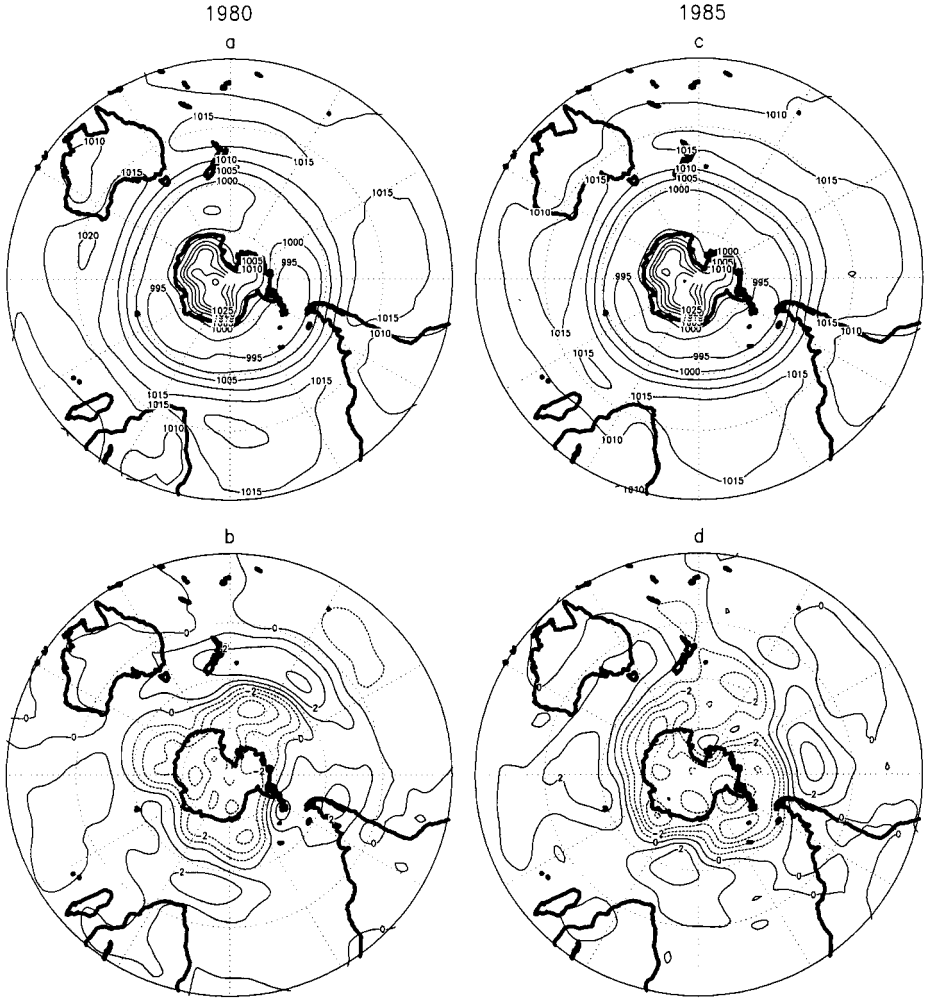

Fig. 7. Sea level pressure (hPa) for the controls of (a) 1980 and (c) 1985, and the perturbations minus the controls for (b) 1980 and (d) 1985. The contour interval in (a) and (c) is 5 hPa. Negative anomalies in (b) and (d) are depicted as dashed contours, and the contour interval is 1 hPa

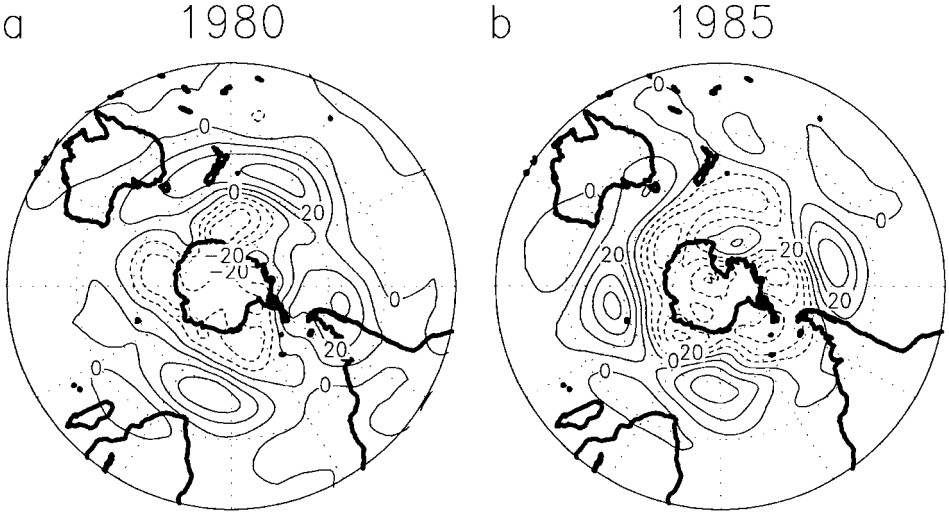

Fig. 8. 500 hPa geopotential height (m) anomalies (perturbations minus the controls) for (a) 1980 and (b) 1985. Negative anomalies are depicted as dashed contours, and the contour interval is 10 m

In contrast, the increase in sea level pressure in the midlatitudes and extending into the subtropics (between 30 and 50° S) (Fig. 7) is associated with 500 hPa height increases (Fig. 8) and 500 hPa temperature increases (not shown) in both years. The increase in mid-tropospheric temperatures (Fig. 5) thus appears to be a consequence of adiabatic warming due to increased subsidence.

The aforementioned changes in sea level pressure and 500 hPa heights are confirmed by changes in vertical velocity (Fig. 9). Firstly, in response to the sea-ice perturbation there is increased subsidence between 40 and 50° S, which, judging from the control and perturbation (not shown) plots, appears to be related to a strengthening and southward extension of the descending limb of the Hadley cell. This result is supported by the sea level pressure changes, where a comparison of the control and perturbation maps in the 2 years (not shown) indicates that the positive sea level pressure anomalies (Fig. 7) are the result of both a strengthening and southward extension of the subtropical high-pressure belt. Secondly, around 60° S there is increased uplift in the ascending limb of the Ferrel cell in response to sea-ice perturbation for both years (Fig. 9), which is associated with the pressure decreases recorded near 60° S (Figs. 7 & 8). The strengthening of this cell extends further south during 1985 compared to 1980, which arguably produces the contrasting results south of 65° S in the 2 years. These results can be related to the temperature response shown previously (Fig. 5). The near-surface temperature change induced by the sea-ice perturbation is greatest at about 57° S in 1980 and at 63° S in 1985, and it is larger for 1985 (Fig. 5). Similarly, increased uplift in the Ferrel cell is centred at about 55° S in 1980 and at 65° S in 1985, and it is more expansive in 1985 (Fig. 9).

In previous studies examining the effect of a change in sea-ice extent, Mitchell & Hills (1986) and Mitchell

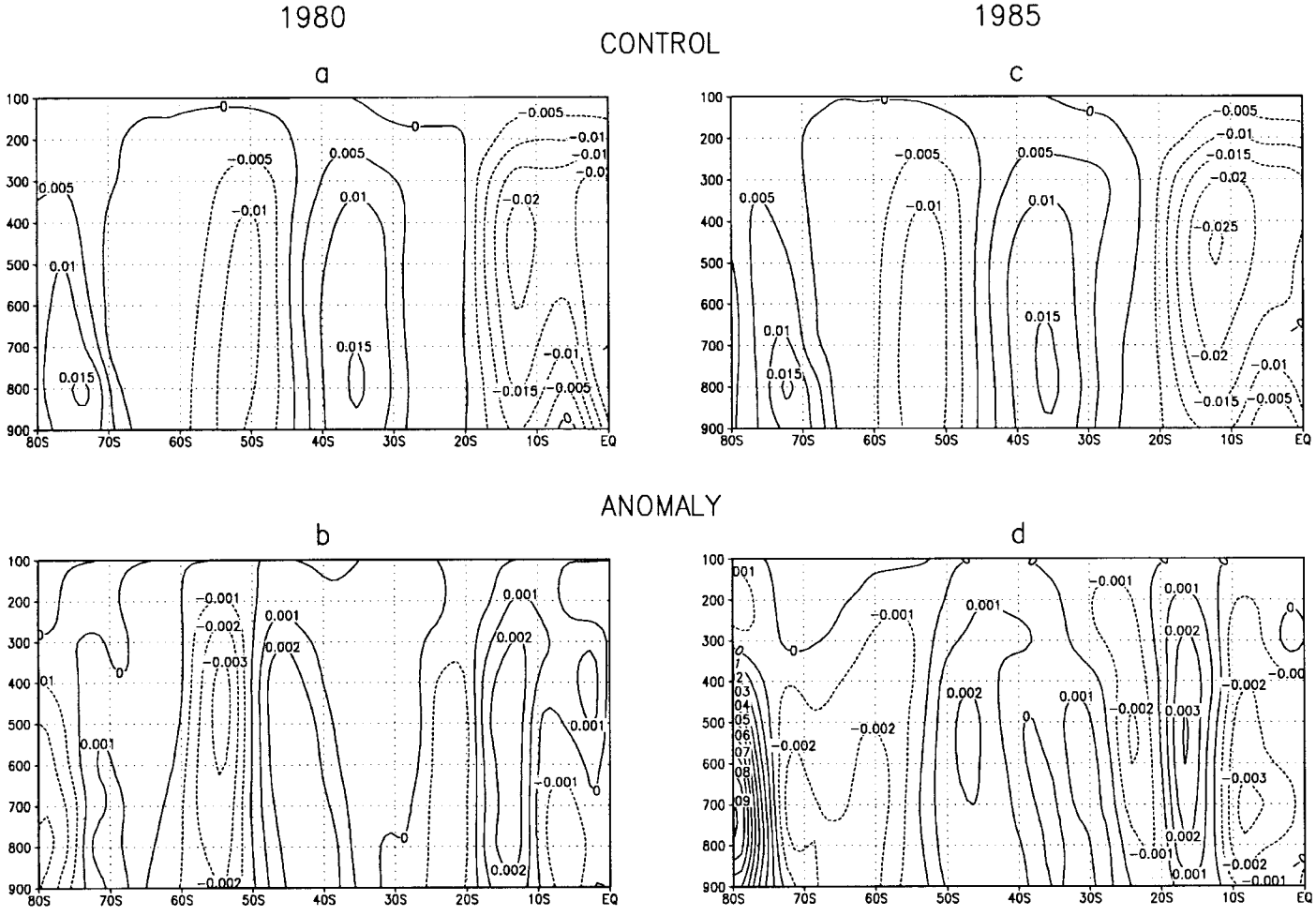

Fig. 9. Vertical cross sections (*y*-axis denotes the pressure level in hPa) of the zonally averaged vertical velocities (Pa s^{-1}) for the (a) control and (b) anomaly (perturbations minus the controls) of 1980 and the (c) control and (d) anomaly of 1985. (Note: Results displayed in the vicinity of the Antarctic plateau are fictitious i.e. below ~700 hPa and poleward of ~75° S. They have been artificially generated by interpolation to pressure levels, even though these levels are below the earth's surface)

& Senior (1989) also found a reduction in surface pressure in the regions from which sea-ice was removed, although the magnitude of the pressure decreases was larger (maximum anomalies of about 10 hPa) than that obtained in the present study (maximum anomalies of about 4 hPa). Both studies also indicated certain areas of sea level pressure increase north of the high-latitude decreases (Mitchell & Hills 1986, Mitchell & Senior 1989). In contrast, Simmonds (1981) and Simmonds & Dix (1987) found both increases and decreases in surface pressure in the regions from which sea-ice was removed, although the spatial distribution of these increases and decreases did not coincide between the studies. It has been suggested that differences in the results of these modelling studies may be due to the different sea-ice anomalies used (Mitchell & Hills 1986, 1987, Mitchell & Senior 1989), the high variability of the model circulation over midlatitude, sub-polar and polar latitudes (Mitchell & Senior 1989) and to differences between the respective models (Mitchell & Hills 1986, 1987, Simmonds & Dix 1987, Mitchell & Senior 1989).

Direct comparisons between the results of the present study and earlier modelling studies investigating the impact of a reduction in Antarctic sea-ice are limited due to the different seasons examined (summer vs winter). Crowley et al. (1994) performed model perturbation experiments to examine the effect of altered Arctic sea-ice and Greenland ice sheet cover on the climate. They commented that the seasonal differences obtained in their study at high latitudes seemed to indicate that the response in summer was a close reflection of the thermal perturbation, whereas the winter response of the atmosphere to the altered temperature field was embedded in the high-latitude flow pattern. Winter is also characterised by more energetic circulation compared to summer, owing to the enhanced equator-pole temperature gradient, and this may result in a stronger, yet more variable, response during this season. Comparisons with previous studies are also limited by differences in GCM resolution, parameterisations and physics; experimental design; and the size and positioning of the imposed anomalies. The modelling studies mentioned previously were performed with earlier generation models of lower horizontal and vertical resolution than used in the present study and significantly larger sea-ice extent anomalies.

5.2. Wind

As expected for summer, the zonal westerlies are strongest near the 200 hPa level at about 45° S in both 1980 and 1985 (Fig. 10). In response to the SST and sea-ice perturbation in both years, there is an increase in wind speeds in the midlatitudes (45 to 65° S) and a decrease in the westerly flow in the subtropics (30 to 40° S) throughout the troposphere (Fig. 10). This response is relatively zonally symmetrical around the hemisphere in both years, as can been seen by the 500 hPa wind speed changes in Fig. 11. The greatest changes are found at the 200 hPa level and the transition between the increase and decrease in wind speeds occurs at about 45° S, where the subtropical jet is located in the control data (Fig. 10). This suggests that there has been a southward shift of the subtropical jet and westerly wind belt and can be seen by examination of the control and perturbation plots (not shown). This southward shift of the jet stream is in agreement with the southward extension of the descending limb of the Hadley cell that was observed for the vertical velocity fields in both years. Streten (1983) analysed the below average ice extent that occurred in the Ross Sea sector in early 1979 (with maximum anomalies during February and March) and showed that the negative ice anomalies were associated with strong westerly midlatitude circulation and ridging from lower latitudes over the eastern portion of the Ross Sea sector. This observation appears to be compatible with the results mentioned above.

It has become clear that the perturbation in both years has resulted in a pattern of alternating bands of positive and negative change extending outwards from the pole, which is evident in both the pressure (sea level pressure and 500 hPa heights) and wind field. The pattern of pressure change obtained in the present study resembles the 'high-latitude' mode, which refers to the pattern of the first sea level pressure and 500 hPa height eigenvectors explaining summer circulation (e.g. Rogers & van Loon 1982, Sinclair et al. 1997). The 'high-latitude' mode is associated with departures around Antarctica which are opposite in sign to those of latitudes equatorward of ~50° S. In the 500 hPa pattern, the eigenvector loadings at lower latitudes over the Pacific and Atlantic Oceans (generally north of 20° S) have the same sign as those around Antarctica, giving a characteristic 'see-saw' pattern between mid- and low/high latitudes (Rogers & van Loon 1982), as is seen in the present study. It has been hypothesised that this pattern suggests that the westerlies tend to strengthen south of 40° S, while they weaken north of 40° S, concurrent with a strengthening of the tropical easterlies, and vice versa (Trenberth 1979). In an examination of pressure anomalies for 40 summer months between 1972 and 1980, Mo & White (1985) also found a pattern of zonally symmetric pressure anomalies, where anomalies in the midlatitudes were negatively correlated with anomalies at low and high latitudes. They suggested that this pat-

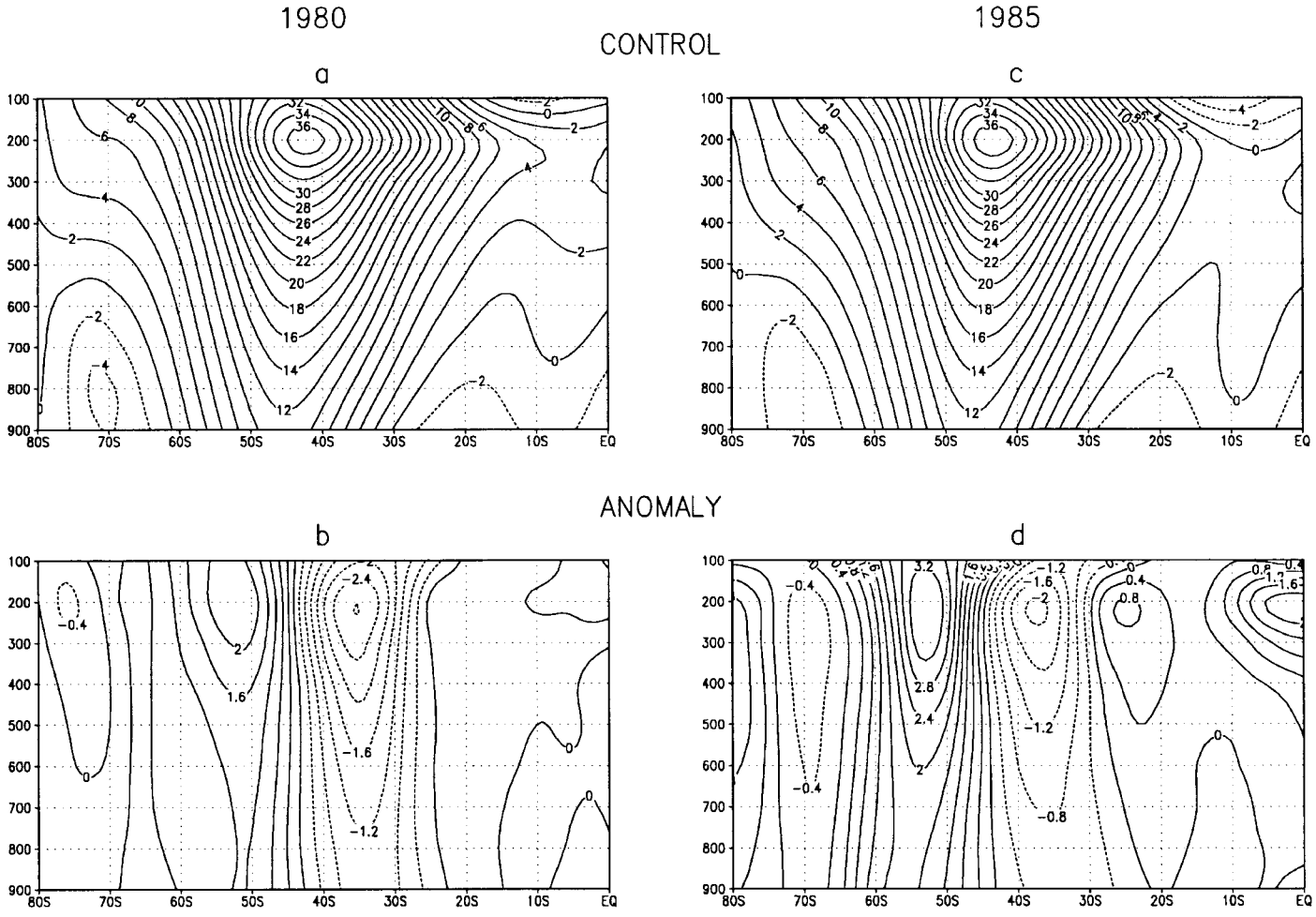

Fig. 10. Vertical cross sections (*y*-axis denotes the pressure level in hPa) of the zonally averaged *u*-component of the wind speed (m s^{-1}) for the (a) control and (b) anomaly (perturbations minus the controls) of 1980 and the (c) control and (d) anomaly of 1985. (Note: Results displayed in the vicinity of the Antarctic plateau are fictitious, i.e. below ~700 hPa and poleward of ~75° S. They have been artificially generated by interpolation to pressure levels, even though these levels are below the earth's surface)

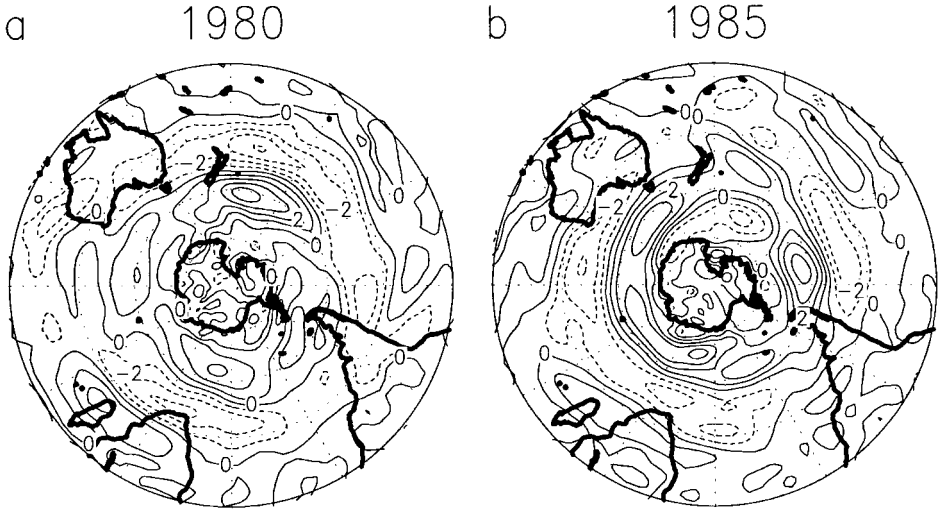

Fig. 11. 500 hPa wind speed (m s^{-1}) anomalies (perturbations minus the controls) for (a) 1980 and (b) 1985. Negative anomalies are depicted as dashed contours, and the contour interval is 1 m s^{-1}

tern may reflect latitudinal shifts in the jet stream. As mentioned previously, the jet stream did shift slightly southwards in the present study, and the 500 hPa wind speed changes match those suggested to be associated with the obtained pattern of pressure change (Trenberth 1979).

The pattern of change could also be explained by the increased ascent near 60° S causing alternating bands of increased ascent and descent. It is suggested that with the exposure of warmer surfaces, due to the sea-ice reduction and SST manipulation south of about 50° S (Figs. 2 & 4), there is a modification of surface fluxes or change in baroclinicity such that increased uplift is favoured. It is likely that it is this increased ascent that is driving the other anomalies of vertical velocity shown on Fig. 9, producing alternating bands of ascent and descent. When this rising air in the region of 60° S reaches the tropopause, it diverges and some moves southward and some northward. The air that is moving northwards would eventually become impeded by air moving poleward in the upward branch of the Hadley cell and would thus subside, producing the increased subsidence that is seen between 30 and 50° S and contributing to a southward extension of the general region of subsidence (Fig. 9). This assertion was examined more closely by looking at the *v*-component (north-south) of the 500 hPa wind (Fig. 12).

Those regions of positive *v*-wind anomalies in Fig. 12 are regions of increased upper level equatorward flow. In both years there are longitudinal bands of increased equatorward flow south of 30° S and these bands coincide with the longitudes of increased pressures between 30 and 50° S (Figs. 7 & 8). For example, in 1985 there is an increase in the 500 hPa equatorward flow south of South Africa, over the eastern Indian Ocean and west of South America (Fig. 12), and there are clear coincident increases in sea level pressure in these 3 specific longitudinal sectors between 30 and 50° S (Fig. 7). This appears to substantiate the hypothesis mentioned above, in that the anomalous rising air near 60° S, shown by the change in vertical velocities and pressure, is transported northwards in the upper troposphere at certain longitudes, resulting in increased subsidence in these sectors between 30 and 50° S. This response is further supported by the results for midlatitude cyclones, where there seems to be a general pattern of density increase at high latitudes, with decreases further north (Fig. 13). In addition, the alternating patterns of *v*-wind anomalies suggest that there may be differences in the amplitudes of the tropospheric Rossby waves at mid- to high-latitudes between the control and perturbation simulations, and that these differences may be manifest in the patterns of midlatitude cyclones.

5.3. Midlatitude cyclones

Midlatitude cyclones are vital for meridional energy transport in the southern hemisphere and arise through baroclinic instability of the mean flow (Trenberth 1991). In the present study, midlatitude cyclones were identified using an automated cyclone identification program, where midlatitude cyclones are defined by the existence of pronounced cyclonic vorticity maxima in the pressure field. The cyclone identification program is based on the algorithm presented in the paper by Murray & Simmonds (1991), and details of the scheme can be found in Hudson & Hewitson (1997) and Hudson (1999).

Frontal cyclogenesis takes place in the midlatitudes, especially where there are strong gradients of SST, and the local meridional temperature gradient appears to be a good indicator of the position of a storm track

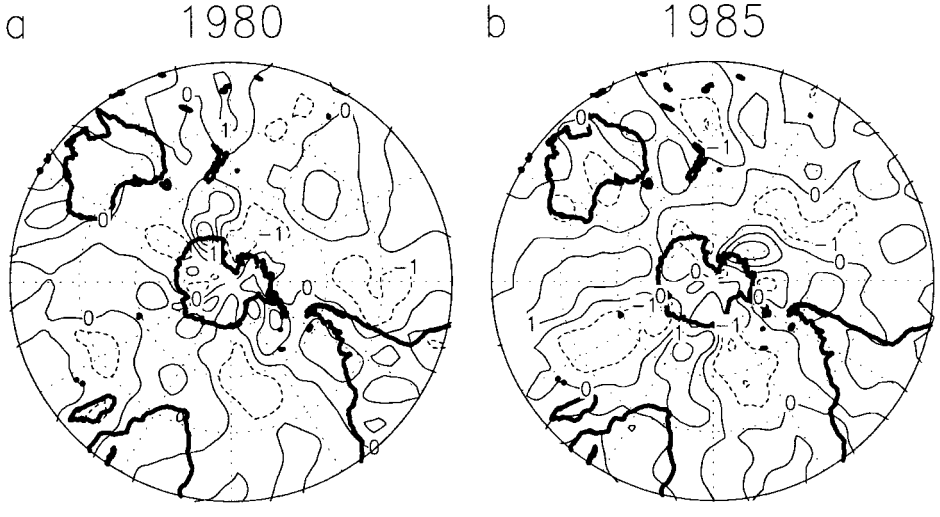

Fig. 12. The *v*-component of the 500 hPa level wind (m s^{-1}) for the perturbations minus the controls in (a) 1980 and (b) 1985. Negative anomalies are depicted as dashed contours, and the contour interval is 1 m s^{-1}

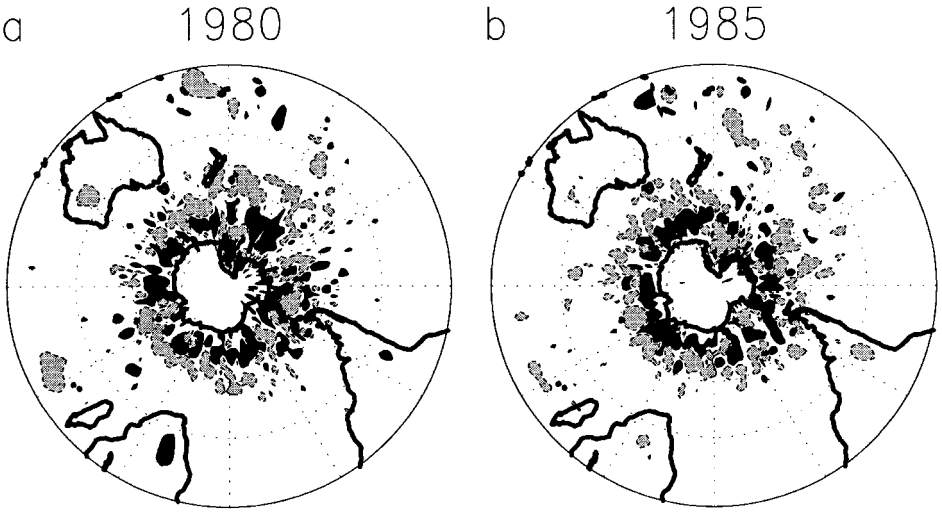

Fig. 13. Midlatitude cyclone density ($\times 10^{-3}$ cyclones [degrees latitude]$^{-2}$) anomalies (perturbations minus the controls) in (a) 1980 and (b) 1985. For clarity, only anomalies greater than 0.4×10^{-3} cyclones (degrees latitude)$^{-2}$ (dark shading) and less than -0.4×10^{-3} cyclones (degrees latitude)$^{-2}$ (light shading) are presented

(Trenberth 1991). In the present study, the SST manipulations caused a decrease in the meridional SST gradient near 50° S in the perturbations compared to the controls (Fig. 14), which could result in reduced baroclinic activity and may account for many of the cyclone density decreases in this zone (Fig. 13). This perhaps best explains the cyclone density change between 30° W and 120° E in both years (Fig. 13). In this sector, the zone of maximum SST increase in the perturbation occurred at 50° S in both years (Fig. 4), thus weakening the meridional temperature gradients near this latitude. Corresponding to this region of relaxed gradients, there is a reduction in cyclone densities in both years (Fig. 13). This region of reduced cyclone densities largely coincides with an increase in sea level pressure (Fig. 7), which extends northwards from about 50° S. The regions of reduced sea level pressure in this sector are largely confined to latitudes south of 50° S (Fig. 7) and thus coincide with the increase in cyclone densities between 60 and 70° S (Fig. 13). This zone corresponds to the sea-ice zone and the latitude band where SST gradients are increased in the perturbations compared to the controls (Fig. 14), which suggests that cyclone densities may have increased due to baroclinic changes and a modification of the surface fluxes caused by the sea-ice reductions.

The relationship between reduced SST gradients and reduced cyclone densities does not, however, seem as clear for the sector north of the Ross Sea. In both years in this region there is an increase in SSTs near 60° S (Fig. 4), suggesting that this is where SST gradients are primarily reduced, and there is also a

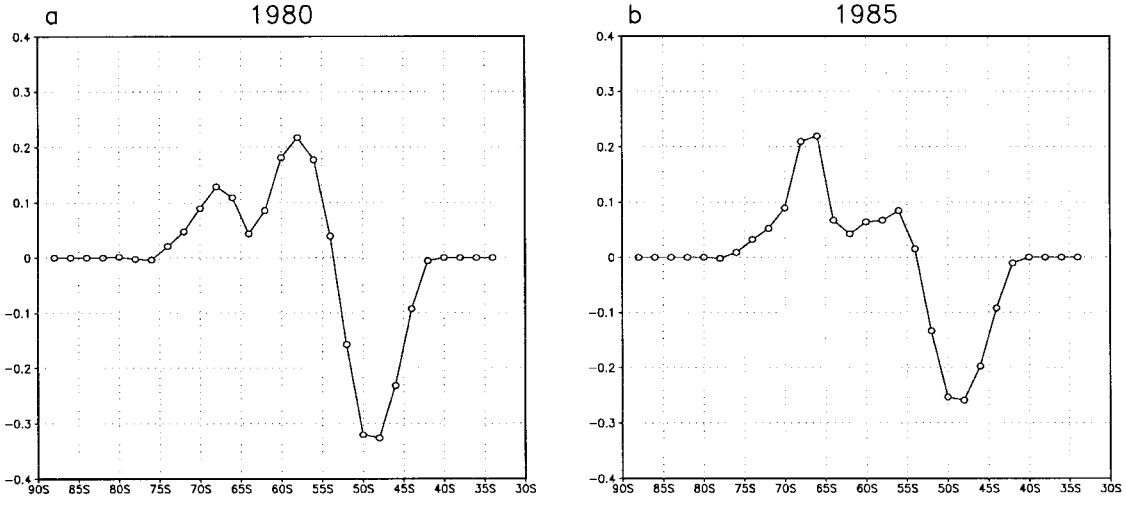

Fig. 14. Change in the SST gradient (K per 3.7° latitude) (calculated for the north-south direction), in terms of the perturbation minus the control for (a) 1980 and (b) 1985

general increase in cyclone densities at this latitude (Fig. 13). This implies that other processes are playing a larger role. South of 55° S, mesocyclone (also referred to as polar lows) cyclogenesis usually dominates over 'synoptic' or frontal cyclogenesis (Carleton & Carpenter 1990). Mesocyclones are vortices that develop in cold air streams (Carleton & Carpenter 1990). They have average diameters of about 3.4° (Carleton 1995); therefore some of the larger mesocyclones may be resolved by the model. It appears that low-level thermal forcing may be an important factor contributing to the development of mesocyclones (Carleton & Carpenter 1990). Therefore, the cyclone density increase north of the Ross Sea may indicate an increase in mesocyclogenesis in response to the increase in surface temperatures. This could also be used as an explanation for the increases in cyclone density apparent at other longitudes in the sea-ice zone (60 to 70° S). Jacobs & Comiso (1993) studied a record decrease in sea-ice extent in the Bellingshausen Sea (62 to 100° W) from mid-1988 through to early 1991. They showed that this decrease coincided with a rise in surface air temperatures on the west side of the Antarctic Peninsula and an increase in cyclonic activity, as was seen in the present study. In addition, a study done by Carleton (1995) for the winter and transition seasons highlighted that a relatively large proportion (approximately 25 to 45%) of mesocyclones develop close to the sea-ice margin, probably in response to baroclinic instability aloft, sea-air interactions and lower-level instability. Carleton (1992) noted that the baroclinicity that is associated with the strong horizontal surface temperature gradients at the sea-ice boundary may enhance mesocyclogenesis even during summer. Thus, with less expansive sea-ice cover in the perturbations, we may expect to see fewer cyclones in the vicinity of the ice margin in the control simulations, and an increase in densities in the region where the margin is located in the perturbation simulations. This may account for some of the cyclone density anomalies around Antarctica.

In modelling experiments where winter sea-ice concentration was reduced, Simmonds & Wu (1993) found a similar pattern of change to the present study. There was also a general increase in cyclone densities at high latitudes, specifically in the band of 10 to 15° latitude width centred on the Antarctic coastline, and fewer to the north of this (Simmonds & Wu 1993). However, studies done with observed data suggest that the potential relationship between Antarctic sea-ice extent and the formation and movement of midlatitude cyclones is largely inconclusive. Godfred-Spenning & Simmonds (1996) examined correlations between the position of the Antarctic sea-ice boundary and midlatitude cyclone density for the period 1973 to 1991. They found that the link between sea-ice and cyclone density was not very strong and tended to be confined to certain regions around the Antarctic coastline. Averaged over the hemisphere, sea-ice extent showed a positive correlation with cyclone density during summer in the region of the sea-ice margin and a negative correlation 5 to 20° north of the sea-ice margin, although the correlations were very small (less than 0.2) (Godfred-Spenning & Simmonds 1996). These results do not seem to be supported by the present study. However, one should be cautious in comparing the results of the correlation study to the present study, since the association between 2 variables in a correlation study does not necessarily imply cause and effect, and correlation analysis considers only linear relationships. Furthermore, the authors conclude that the forcing of sea-ice extent by the atmosphere is a more dominant factor than sea-ice affecting cyclone density (Godfred-Spenning & Simmonds 1996), and the former is not considered in the present study.

Howarth (1983) also found little correlation between sea-ice and cyclone tracks on a hemispheric scale in a study of the period 1973 to 1975. He suggested that the shape of Antarctica, and thus maybe the continental-ice/sea-ice boundary, is more important in determining the longitudinal position of cyclone tracks. However, Howarth (1983) does not eliminate the possibility that the sea-ice margin may influence cyclone movements, but proposes that this may be restricted to short time periods and specific locations. It has been repeatedly stated that it is unclear how Antarctic sea-ice extent, which undergoes an annual cycle of contraction and expansion, can directly affect the position of midlatitude cyclones, which experience a semi-annual oscillation in latitudinal position (e.g. van Loon 1967, Howarth 1983, Carleton 1992). However, it has been shown that the semi-annual oscillation is not that apparent when considering patterns of cyclogenesis (Budd 1982), since the latitude of maximum cyclogenesis is located furthest north in September and furthest south in March (Carleton 1992). Therefore, the formation of new midlatitude cyclones may be related to sea-ice advance and retreat (Carleton 1992).

Sinclair et al. (1997) examined the relationship between the leading modes of sea level pressure variability and cyclone activity. They found that the first sea level pressure EOF (empirical orthogonal function), which is the previously mentioned 'high-latitude mode', modulates cyclone activity between high and midlatitudes. When there are increased (decreased) westerlies in the region 55 to 65° S, then there are more (fewer) cyclones in the circumpolar regions and fewer (more) in mid- and lower latitudes (Sinclair et al. 1997). This result agrees with the present study, where a general increase in westerly flow between 45 and 65° S

is associated with a general increase in cyclone densities between 60 and 70° S and a decrease further north (40 to 60° S).

5.4. 500 hPa seasonal wave number 1

It has been suggested that the long waves in the southern hemisphere are primarily forced by orographic and thermal forcing associated with the zonal asymmetries of Antarctica (Anderssen 1965, Grose & Hoskins 1979, Trenberth 1980, Karoly 1985, James 1988, Simmonds et al. 1989). Wave number 1 has been identified as being the most dominant component of the climatological mean geopotential height field in the southern hemisphere (van Loon & Jenne 1972, Quintanar & Mechoso 1995). Wave numbers 2 and 3, as well as the shorter waves, contribute less to the quasi-stationary field, because they have larger phase velocities, and thus their position around the hemisphere is more variable (van Loon & Jenne 1972, Quintanar & Mechoso 1995).

One-dimensional Fourier analysis of the seasonally averaged 500 hPa heights along latitude circles was used in the present study to examine wave number 1. Wave number 1 is largest at high to midlatitudes and peaks near 57° S in 1980 and near 50° S in 1985 (Fig. 15). In the perturbations, there is a reduction in the amplitude of the peaks in both years, especially in 1985 (Fig. 15). Anderssen (1965) has suggested that the existence of wave number 1 may be due to thermal effects associated with the asymmetric SST distribution around Antarctica. In order to investigate the possible influence of the SST distribution on wave number 1, the control and perturbation SSTs at 54° S (midway between the peaks of the 2 years) were examined for both years and are shown in Fig. 16. As has been found by other researchers, the position of the trough of wave number 1 at this latitude occurs near 20° E in both years (not shown), which coincides with the region of coldest SSTs (Fig. 16). In other words, wave number 1 has the same asymmetric distribution about the pole as the SST distribution, in that the trough (ridge) is located over the African (Pacific) sector, where the SST distribution as manifested by the Antarctic Convergence is located furthest north (south). The manipulation of SSTs in the experiment resulted in a reduction of the asymmetry of the SSTs at 54° S (Fig. 16), and this may therefore partially account for the reduced amplitude of wave number 1 (Fig. 15). In addition, Trenberth (1980) found that the relationship between wave number 1 and the zonal westerlies is such that if the westerlies are stronger in the midlatitudes and weaker to the north and south, then the amplitude of wave number 1 tends to be smaller than usual. This corresponds with the results from the present study.

6. CONCLUSION

This paper considers the response of an atmospheric GCM to a reduction in Antarctic sea-ice extent during summer. Sea-ice and SST perturbations were applied to the summers of 1980 and 1985 and the response over the southern hemisphere was investigated. Even though the perturbations are relatively small, the results are cohesive and physically plausible, and the perturbations elicit a fairly consistent response between the 2 years. This suggests that the results obtained are relatively robust and in most cases represent a true sea-ice-atmosphere signal rather than vari-

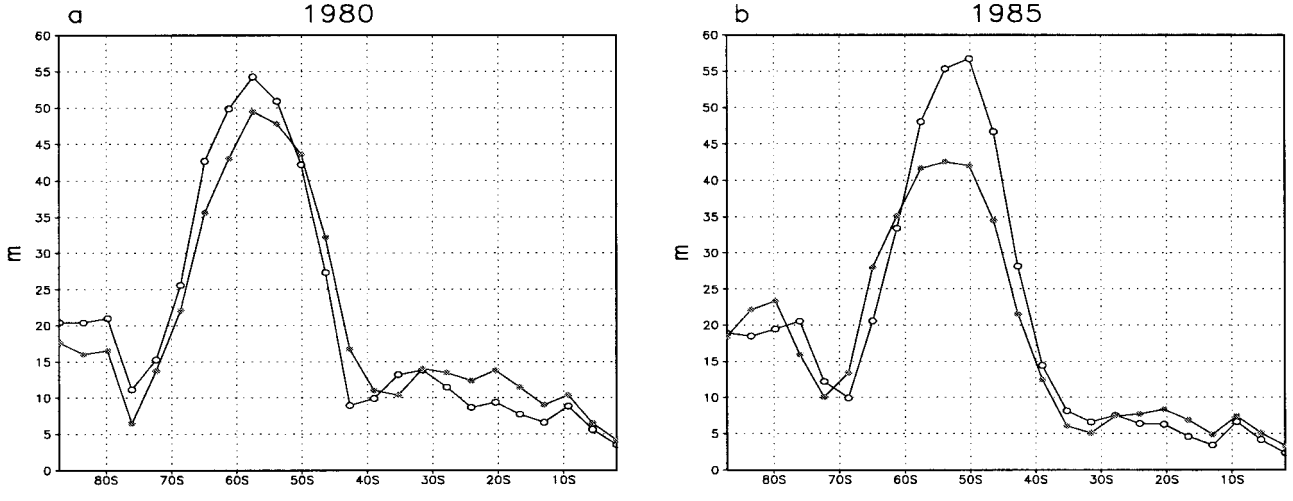

Fig. 15. Amplitude (m) of seasonal wave number 1 for the control (s) and perturbation (d) data in (a) 1980 and (b) 1985

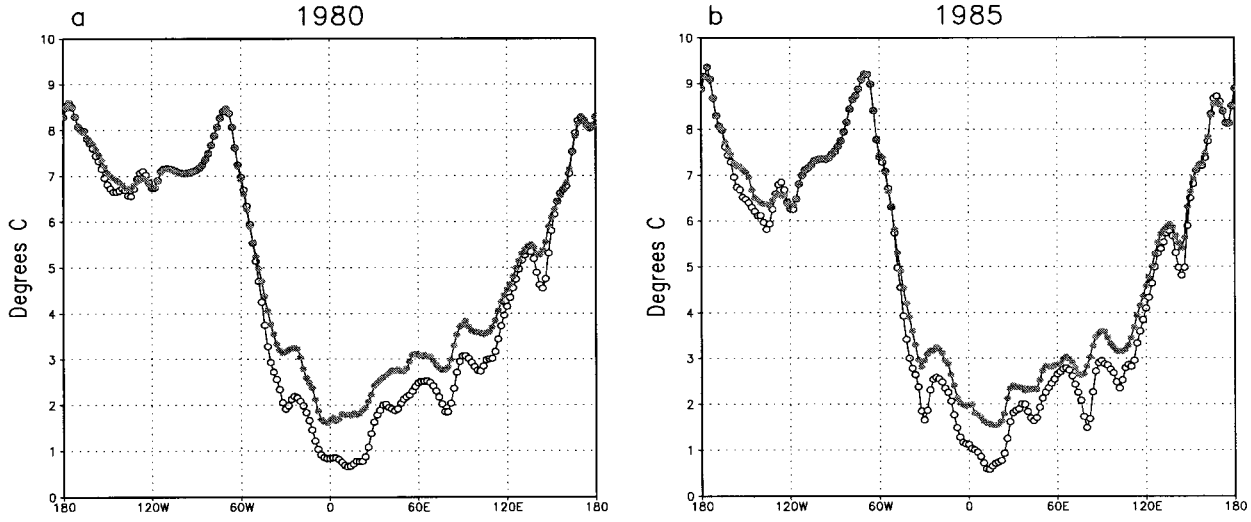

Fig. 16. SST (°C) distribution for the control (s) and perturbation (d) data at 54° S in (a) 1980 and (b) 1985

ance due to natural variability. It would be advantageous in future studies to use much larger ensembles of GCM simulations in order to help detect a definitive sea-ice - atmosphere signal above the noise. Differences between 1980 and 1985 can probably be ascribed to the slightly different sea-ice and SST anomalies used, differences in their control sea-ice extent and the high variability of circulation at middle and high latitudes. The major findings of the response to the perturbation are summarised below:

- The atmospheric response over the southern hemisphere is to some degree sensitive to the positioning and magnitude of the introduced SST and sea-ice anomalies.
- There are increases in surface air temperature around Antarctica which largely correspond to the regions of SST increase in the perturbation simulation. Consequently, the largest increases are found in the Weddell and Ross Sea sectors.
- The zonally averaged vertical velocities show increased uplift in the region of 60° S and increased subsidence between 30 and 50° S. The results suggest that the increased subsidence between 40 and 50° S is caused by a strengthening and slight southward extension of the descending limb of the Hadley cell.
- There are corresponding regions of sea level pressure and 500 hPa height decrease around Antarctica (50 to 60° S). The pattern of decrease is clearly related to the pattern of surface temperature increase around Antarctica.
- There are corresponding regions of sea level pressure and 500 hPa height increase between 30 and 50° S.
- There are increases in tropospheric wind speeds in mid- to high latitudes (45 to 65° S) and decreases in the subtropics (30 to 40° S). The pressure changes appear to have induced a slight southward shift of the jet stream.
- There is a general decrease in cyclone densities between 40 and 60° S and an increase in densities between 60 and 70° S.
- There is a general reduction in the peak amplitude of seasonal wave number 1, which may be partly due to reduced SST and sea-ice asymmetries about the pole.

It is important to remember that this study does not consider the feedback from the atmosphere to the ocean and ice. 'The sea-ice/atmosphere relationship is mutual and reciprocal' (Hanna 1996, p. 382), and there are complex interactions involved. The present study used prescribed sea-ice and SSTs so that the impact of the sea-ice anomalies on the climate could be studied in a controlled manner. This is, however, a simplification and the presence of full sea-ice and ocean models could modify the results.

A limitation of the present study that stems from using prescribed SST and sea-ice fields is the crude treatment of sea-ice thickness, which is set as a linear function of latitude (Pollard & Thompson 1995b). Improvement of the handling of this parameter would facilitate interesting experiments where sea-ice thickness could be perturbed. In addition, in the future, longer simulations with reduced sea-ice, perhaps 10 yr in duration, would allow the research of lower-frequency and longer-term responses to the perturbation, for example, as to whether a reduced Antarctic sea-ice extent could affect the El Niño Southern Oscillation, or

the Semi-Annual Oscillation. Performing the simulations in different years would also help to resolve the variability of the atmospheric response.

The ocean and sea-ice may play important roles in the evolution of atmospheric anomalies, producing smaller or larger effects than are seen in the present study. Thus, the present study is not a forecast of the real climatic changes that would occur if sea-ice cover was less than normal, but is rather an initial attempt to identify key processes and the sensitivity of the atmosphere to sea-ice changes. The present study has highlighted that the atmosphere is sensitive to fairly small changes in sea-ice extent, and this reinforces the need for better sea-ice models in fully coupled ocean-atmosphere GCMs. The IPCC (1996) notes that a common problem with coarse resolution coupled GCMs is that the sea-ice edge in the Antarctic is too far poleward. Results from the present research suggest that errors in sea-ice extent, as simulated by sea-ice models, may distort atmospheric circulation. This paper increases our understanding of sea-ice - atmosphere interactions, as well as providing an indication of the influence that negative sea-ice anomalies may have on the climate, in the context of interannual differences in sea-ice extent, as well as the reduction in sea-ice that may occur in the future as a consequence of anthropogenically induced global warming.

Acknowledgements. The Earth Systems Science Center at Penn State University and the National Center for Atmospheric Research, Colorado, are gratefully acknowledged for allowing access to the GENESIS GCM. Thanks are also due to 3 anonymous reviewers for their helpful comments on this paper.

Appendix 1. The sea-ice algorithm

The algorithm is designed for perturbation studies using GCMs run with prescribed SSTs and sea-ice extent. It relies on the analysis of observed sea-ice coverage in order to obtain the anomalous SST and sea-ice data set. The observed data set in the present study is that which is used for the AMIP control simulation with the GENESIS model, and is the COLA (Center for Ocean, Land and Atmosphere)/CAC (Climate Analysis Center) AMIP SST and sea-ice data set (Reynolds & Roberts 1987, Reynolds 1988). It is a 10 yr observational data set, based on a 2° latitude-longitude grid, and contains 2 data arrays for each month of the period from January 1979 to December 1988. The first array is a sea-ice mask, where a grid cell is either 1 or 0, denoting ice or ocean respectively, and the second array is the SSTs. In the algorithm, grid-cell-specific melt/freeze indicators are determined for each month of the observed data and are then used as a basis for exacerbating the melt or diminishing the freeze. For any given month of the observed data, the algorithm will produce a corresponding month with reduced sea-ice coverage which can be input into the model.

The flow chart in Fig. 17 shows the general procedure used in the creation of the perturbation sea-ice data set, including the decision criterion used to determine whether a particular grid cell in a certain month should remain as ice or be changed to water. The procedure is carried out for every sea-ice grid cell in each month of the observed data (AMIP SST and sea-ice data) for which a corresponding month with reduced sea-ice limits is required. The first stage is to loop through the observational data set and for each month determine previous, current and future states for each grid cell. 'Previous' refers to the month prior to the month under consideration and 'future' refers to the month following the month under consideration. In this context, the 'state' of a grid cell is the number of the 8 surrounding grid cells that are water. These previous, current and future state values are thus an indication of the degree to which the center grid cell in question is surrounded by water or ice. A value greater (smaller) than 4 implies that water (ice) is the dominant phase. The decision criterion of whether or not to alter a grid cell from ice to water differs depending on whether the month falls in a general melting or freezing trend (Fig. 17). In both cases, the 8 surrounding grid cells of the cell under consideration are examined in order to determine

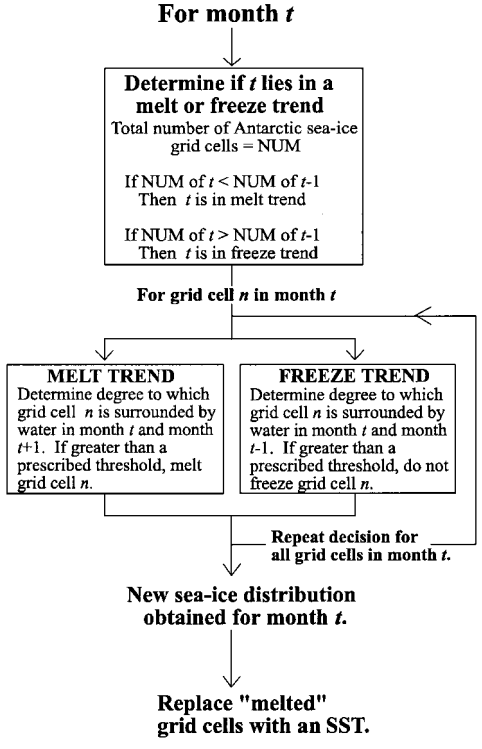

Fig. 17. A flow chart showing the procedures involved in the creation of a perturbation sea-ice data set, where the sea-ice limits are smaller than the corresponding control sea-ice data. The algorithm is applied to each grid cell of each month of the control sea-ice data in order to create the new sea-ice distribution. The control sea-ice and the new sea-ice data (with a reduced sea-ice extent) can then be used in GCM sensitivity simulations

the degree to which it is surrounded by water (i.e. the current state value). However, should the month fall in a melting trend, then the degree to which the grid cell is surrounded by water is examined in both the month under examination (t) (current state value) and the future month (t+1) (future state value). It is desirable to 'melt' those grid cells in the current month (t) that have a greater chance of melting in the future month. Therefore, those grid cells that are largely surrounded by water in months t and t+1 are changed from ice to water.

On the other hand, if the month falls in a freezing trend, then the degree to which the grid cell is surrounded by water is examined in both the month under examination (t) and the previous month (t – 1). The rationale behind this is that those grid cells which are largely surrounded by water in the previous month are less likely to freeze in the following month compared to those that are surrounded by relatively more ice. It is desirable to melt those grid cells which, although they froze in the observed data in month t, had a fairly low chance of freezing, as is shown by the degree of influence of water in month (t – 1). Therefore, those grid cells that are largely surrounded by water in months t and (t – 1) are changed from ice to water.

The examination of the previous and future months (for freezing and melting trends respectively), as well as the month under consideration, allows one to take into account the observed asymmetrical melting around Antarctica. For example, in a certain region the future state value may be more inclined towards water than the current state value, due to melting taking place from the current month to the future month. However, this may not be the case in a different region which could be more resistant to melting at that time of year.

The thresholds that are used to determine whether the degree of 'influence' of water is sufficient to allow alteration of the value of a grid cell are the values of 3 constants, PST, CST and FST. PST, CST and FST are set for comparison with the previous state value, the current state value and the future state value of a grid cell respectively. The constants are set at a default value of 3. In a particular month, for each grid cell that is ice the melt rule is as follows: if the current state value is greater than the value of CST or if the future state value is greater than FST, then the grid cell is 'melted'. This implies that if in the future or current month (future state value and current state value) there are more than 3 (the default) surrounding grid cells that are water (i.e. fewer than 5 grid cells are ice) then the central grid cell, of the current month is changed from ice to water. If the condition does not hold true, then the grid cell is left as ice. Similarly, if the month falls in a freezing trend, a grid cell's value is altered if its previous state value is greater than PST or if its current state value is greater than CST. The constants are set at a default value of 3, so that 'melting' will only occur if at least half of the surrounding grid cells are water. The decision procedure of whether or not to change the value of a grid cell is repeated for every sea-ice cell of the observed data such that a new sea-ice distribution, with reduced sea-ice limits, is obtained for the particular month.

The algorithm also incorporates 3 possible ways of obtaining perturbations of differing strengths. Firstly, the algorithm can be executed in an iterative procedure, such that the greater the number of iterations the larger the perturbation. In subsequent iterations, the calculations are based on the perturbed ice extent obtained at the end of the previous iteration. Secondly, the values of the constants can be altered. If the value of the constants is decreased, then the conditions for changing a grid cell's value are less stringent. For example, if the values of CST and FST are decreased from 3 to 2, then in the case of a melting trend, if more than 2 surrounding grid cells are water (i.e. fewer than 6 grid cells are ice) in the future or current month, the central grid cell of the current month is changed from ice to water. Lastly, perturbations intermediate between the control and a specified perturbation, e.g. that produced with default settings, can be obtained by selecting a fractional position (f) between the 2 data sets. For example, if f is set to 0.5, then for each longitude of every month the new ice edge is positioned halfway between the control and the specified perturbation. The sea-ice perturbation used in the present study was created with PST = CST = FST = 3, 1 iteration and f = 0.45.

Before the perturbed ice-field can be introduced into a GCM, the SSTs need to be adjusted. SSTs are assigned to those new ice-free ocean areas and the temperature field is extended to the new ice boundary. In the algorithm, SSTs poleward of the 4°C isotherm are increased using interpolation procedures, so that the SST field is 'stretched' to the new sea-ice boundary. The 4°C isotherm was chosen subjectively, owing to minimal seasonal movements of the isotherm apparent from the observed data. This method of SST manipulation is preferable to replacing the removed ice with a single ocean temperature, as has been done in some other similar simulations (e.g. Mitchell & Hills 1986, Mitchell & Senior 1989, Crowley et al. 1994), since it better resembles the observed change in the SST field when sea-ice extent changes, and a SST gradient extending to the ice boundary is retained. A more detailed description of the SST adjustment and the algorithm in general is provided by Hudson (1999).

LITERATURE CITED

Ackley SF (1981) A review of sea-ice weather relationships in the Southern Hemisphere. In: Allison I (ed) Sea level, ice, and climatic change. Proceedings of the Canberra Symposium, December 1979. International Association of Hydrological Sciences (IAHS) Press, Wallingford, IAHS Publication No. 131, p 127–159

Ackley SF, Keliher TE (1976) Antarctic sea-ice dynamics and its possible climatic effects. AIDJEX Bull 33:53–76

Anderssen EC (1965) A study of atmospheric long waves in the Southern Hemisphere. Notos 14:57–65

Barron EJ, Peterson WW, Pollard D, Thompson SL (1993) Past climate and the role of ocean heat transport: model simulations for the Cretaceous. Paleoceanography 8:785–798

Barron EJ, Fawcett PJ, Peterson WW, Pollard D, Thompson SL (1995) A 'simulation' of mid-Cretaceous climate. Paleoceanography 10:953–962

Budd WF (1982) The role of Antarctica in southern hemisphere weather and climate. Aust Meteorol Mag 30:265–272

Budd WF (1991) Antarctica and global change. Clim Change 18:271–299

Carleton AM (1981) Ice-ocean-atmosphere interactions at high southern latitudes in winter from satellite observation. Aust Meteorol Mag 29:183–195

Carleton AM (1992) Synoptic interactions between Antarctica and lower latitudes. Aust Meteorol Mag 40:129–147

Carleton AM (1995) On the interpretation and classification of

mesoscale cyclones from satellite infrared imagery. Int J Remote Sensing 16(13):2457–2485
Carleton AM, Carpenter DA (1990) Satellite climatology of 'polar lows' and broadscale climatic associations for the southern hemisphere. Int J Climatol 10:219–246
Crowley TJ, Baum SK (1994) General circulation model study of late Carboniferous interglacial climates. Palaeoclimates 1:3–21
Crowley TJ, Baum SK, Kim KY (1993) General circulation model experiments with pole-centered supercontinents. J Geophys Res 98:8793–8800
Crowley TJ, Yip KJJ, Baum SK (1994) Effect of altered Arctic sea ice and Greenland ice sheet cover on the climate of the GENESIS general circulation model. Global Planet Change 9:275–288
Crowley TJ, Yip KJJ, Baum SK, Moore SB (1996) Modelling Carboniferous coal formation. Paleoclimates 2:159–177
Dümenil L, Schröder S (1989) The impact of an ice-free Arctic Ocean on the general circulation in winter. In: Boer GJ (ed) Research activities in atmospheric and oceanic modelling. CAS/JSC Working Group on Numerical Experimentation Report 13. WMO/TD 332, World Meteorological Organisation, Geneva, p 7.42–7.43
Fletcher JO, Mintz Y, Arakwa A, Fox T (1973) Numerical simulation of the influence of Arctic sea ice on climate. In: Proceedings of the IAMAP/IAPSO/SCAR/WMO symposium on energy fluxes over polar surfaces (Moscow, August 1971). WMO Tech. Note No. 129, World Meteorological Organisation, Geneva, p 181–218
Foley JA (1994) The sensitivity of the terrestrial biosphere to climatic change: a simulation of the middle Holocene. Glob Biogeochem Cycles 8:505–525
Gates WL (1992) AMIP: The Atmospheric Model Intercomparison Project. Bull Am Meteorol Soc 73(12):1962–1970
Godfred-Spenning CR, Simmonds I (1996) An analysis of Antarctic sea-ice and extratropical cyclone associations. Int J Climatol 16:1315–1332
Grose WL, Hoskins BJ (1979) On the influence of orography on the large-scale atmospheric flow. J Atmos Sci 36: 223–234
Hanna E (1996) The role of Antarctic sea ice in global climate change. Prog Phys Geogr 20:371–401
Herman GF, Johnson WT (1978) The sensitivity of the general circulation to Arctic sea ice boundaries: a numerical experiment. Mon Weather Rev 106:1649–1664
Howarth DA (1983) An analysis of the variability of cyclones around Antarctica and their relationship to sea-ice extent. Ann Assoc Am Geogr 73(4):519–537
Hudson DA (1997) Southern African climate change simulated by the GENESIS GCM. S Afr J Sci 93(9):389–403
Hudson DA (1999) Antarctic sea-ice extent, southern hemisphere circulation and South African rainfall. PhD thesis, University of Cape Town
Hudson DA, Hewitson BC (1997) Midlatitude cyclones south of Africa in the GENESIS GCM. Int J Climatol 17:459–473
Intergovernmental Panel on Climate Change (IPCC) (1996) Climate change 1995—the science of climate change. Contribution of Working Group 1 to the Second Assessment Report of the Intergovernmental Panel on Climate Change. Houghton JT, Meira Filho LG, Callander BA, Harris N, Kattenberg A, Maskell K (eds) Cambridge University Press, Cambridge
Jacobs SS, Comiso JC (1993) A recent sea-ice retreat west of the Antarctic peninsula. Geophys Res Lett 20(12): 1171–1174
James IN (1988) On the forcing of planetary-scale Rossby waves by Antarctica. Q J R Meteorol Soc 114:619–637
Jenkins G (1995) Early earth's climate: cloud feedback from reduced land fractions and ozone concentrations. Geophys Res Lett 22:1513–1516
Karoly DJ (1985) An atmospheric climatology of the southern hemisphere based on ten years of daily numerical analyses (1972–82): II Standing wave climatology. Aust Meteorol Mag 33:105–116
Ledley TS (1988) For a lead-temperature feedback in climatic variation. Geophys Res Lett 15(1):36–39
Mayes PR (1985) Secular variations in cyclone frequencies near the Drake Passage, Southwest Atlantic. J Geophys Res 90:5829–5939
Mitchell JFB, Hills TS (1986) Sea-ice and the antarctic winter circulation: a numerical experiment. Q J R Meteorol Soc 112:953–969
Mitchell JFB, Hills TS (1987) Reply to comment by Simmonds and Dix on 'Sea-ice and the antarctic winter simulation: a numerical experiment' by J.F.B. Mitchell and T.S. Hills. Q J R Meteorol Soc 113:1401–1403
Mitchell JFB, Senior CA (1989) The antarctic winter; simulations with climatological and reduced sea-ice extents. Q J R Meteorol Soc 115:225–246
Mo KC, White GH (1985) Teleconnections in the Southern Hemisphere. Mon Weather Rev 113:22–37
Murray RJ, Simmonds I (1991) A numerical scheme for tracking cyclone centres from digital data. Part 1: development of the scheme. Aust Meteorol Mag 39:155–166
Murray RJ, Simmonds I (1995) Responses of climate and cyclones to reductions in Arctic winter sea ice. J Geophys Res 100:4791–4806
Newson RL (1973) Response of a general circulation model of the atmosphere to removal of the arctic ice-cap. Nature 241:39–40
Nicholls N (1996) Modelling climate variability. In: Giambelluca TW, Henderson-Sellers A (eds) Climate change. Developing southern hemisphere perspectives. John Wiley & Sons, Chichester, p 131–143
Otto-Bliesner BL (1993) Tropical mountains and coal formation: a climate model study of the Westphalian (306 Ma). Geophys Res Lett 20:1947–1950
Pollard D, Thompson SL (1994) Sea-ice dynamics and CO_2 sensitivity in a global climate model. Atmos Ocean 32(2): 449–467
Pollard D, Thompson SL (1995a) Use of a land-surface-transfer scheme (LSX) in a global climate model: the response to doubling stomatal resistance. Global Planet Change 10: 129–161
Pollard D, Thompson SL (1995b) Users' guide to the GENESIS Global Climate Model Version 2.0. Interdisciplinary Climate Systems Section, Climate and Global Dynamics Division, National Center for Atmospheric Research, Boulder, CO
Quintanar AI, Mechoso CR (1995) Quasi-stationary waves in the Southern Hemisphere. Part I: Observational data. J Clim 8:2659–2672
Raymo ME, Rind D, Ruddiman WF (1990) Climatic effects of reduced Arctic sea ice limits in the GISS II general circulation model. Paleoceanography 5(3):367–382
Reynolds RW (1988) A real-time global sea surface temperature analysis. J Clim 1:75–86
Reynolds RW, Roberts L (1987) A global sea surface temperature climatology from in situ, satellite and ice data. Trop Ocean-Atmos Newsl 37:15–17 (available from Rosentiel School of Marine and Atmospheric Science, Miami, FL)
Rogers JC, van Loon H (1982) Spatial variability of sea level pressure and 500 mb height anomalies over the Southern Hemisphere. Mon Weather Rev 110:1375–1392

Royer JF, Planton S, Déqué M (1990) A sensitivity experiment for the removal of Arctic sea ice with the French spectral general circulation model. Clim Dyn 5:1–17

Serafini YV, Le Treut H (1988) Modélisation des climats extrêmes: impact sur le climat d'une fonte des glaces Arctiques. Note Interne LMD no. 144, Laboratoire de Météorologie Dynamique, Paris

Simmonds I (1981) The effect of sea-ice on a general circulation model of the Southern Hemisphere. In: Allison I (ed) Sea level, ice, and climatic change. Proceedings of the Canberra Symposium, December 1979. International Association of Hydrological Sciences (IAHS) Press, Wallingford, IAHS Publication No. 131, p 193–206

Simmonds I, Budd WF (1990) A simple parameterization of ice leads in a General Circulation Model, and the sensitivity of climate to change in Antarctic ice concentration. Ann Glaciol 14:266–269

Simmonds I, Budd WF (1991) Sensitivity of southern hemisphere circulation to leads in the Antarctic pack ice. Q J R Meteorol Soc 117:1003–1024

Simmonds I, Dix M (1987) Comments on paper 'Sea-ice and the antarctic winter circulation: a numerical experiment' by J.F.B. Mitchell and T.S. Hills, 1986. Q J R Meteorol Soc 113:1396–1401

Simmonds I, Wu X (1993) Cyclone behaviour response to changes in winter southern hemisphere sea-ice concentration. Q J R Meteorol Soc 119:1121–1148

Simmonds I, Dix M, Rayner P, Trigg G (1989) Local and remote response to zonally uniform sea-surface temperature in a July general circulation model. Int J Climatol 9:111–131

Sinclair MR, Renwick JA, Kidson JW (1997) Low-frequency variability of Southern Hemisphere sea level pressure and weather system activity. Mon Weather Rev 125:2531–2543

Streten NA (1983) Antarctic sea ice and related atmospheric circulation during FGGE. Arch Meteorol Geophys Bioklimatol Ser A 32:231–246

Thompson SL, Pollard D (1995) A global climate model (GENESIS) with a land-surface-transfer scheme (LSX). Part 1: Present-day climate. J Clim 8:732–761

Thompson SL, Pollard D (1997) Greenland and Antarctic mass balances for present and doubled atmospheric CO_2 from the GENESIS Version-2 Global Climate Model. J Clim 10(5):871–900

Trenberth KE (1979) Interannual variability of the 500 mb zonal mean flow in the Southern Hemisphere. Mon Weather Rev 107:1515–1524

Trenberth KE (1980) Planetary waves at 500 mb in the Southern Hemisphere. Mon Weather Rev 108:1378–1389

Trenberth KE (1991) Storm tracks in the Southern Hemisphere. J Atmos Sci 48:2159–2178

van Loon H (1967) The half-yearly oscillations in middle and high southern latitudes and the coreless winter. J Atmos Sci 24:472–486

van Loon H, Jenne RL (1972) The zonal harmonic standing waves in the Southern Hemisphere. J Geophys Res 77: 992–1003

Warshaw M, Rapp RP (1973) An experiment on the sensitivity of a global circulation model. J Appl Meteorol 12:43–49

Watkins AB, Simmonds I (1995) Sensitivity of numerical prognoses to Antarctic sea ice distribution. J Geophys Res 100: 22681–22696

Editorial responsibility: Brent Yarnal, University Park, Pennsylvania, USA

Submitted: October 19, 1999; Accepted: April 26, 2000
Proofs received from author(s): November 2, 2000